

Bayesian Nonparametric Higher Order Hidden Markov Models

Abhra Sarkar

Department of Statistics and Data Sciences, University of Texas at Austin,
2317 Speedway D9800, Austin, TX 78712-1823, USA
abhra.sarkar@utexas.edu

and

David B. Dunson

Department of Statistical Science, Duke University,
Box 90251, Durham NC 27708-0251
dunson@duke.edu

Abstract

We consider the problem of flexible modeling of higher order hidden Markov models when the number of latent states and the nature of the serial dependence, including the true order, are unknown. We propose Bayesian nonparametric methodology based on tensor factorization techniques that can characterize any transition probability with a specified maximal order, allowing automated selection of the important lags and capturing higher order interactions among the lags. Theoretical results provide insights into identifiability of the emission distributions and asymptotic behavior of the posterior. We design efficient Markov chain Monte Carlo algorithms for posterior computation. In simulation experiments, the method vastly outperformed its first and higher order competitors not just in higher order settings, but, remarkably, also in first order cases. Practical utility is illustrated using real world applications.

Some Key Words: Bayesian nonparametrics, Conditional tensor factorization, Higher order hidden Markov models.

Short Title: Higher Order Hidden Markov Models

1 Introduction

Hidden Markov models (HMMs) have been tremendously successful in statistical analyses of sequentially generated data in diverse areas like speech recognition (Rabiner, 1989; Fox *et al.*, 2008), proteomics (Bae *et al.*, 2005; Lennox *et al.*, 2010), genomics (Guha *et al.*, 2008a; Yau *et al.*, 2011), and economics and finance (Hamilton, 1990; Albert and Chib, 1993).

The basic HMM consists of two processes: a *hidden* process $\{c_t\}$, which evolves according to a first order Markov chain with discrete state space, and a potentially multivariate *observed* process $\{\mathbf{y}_t\}$ observed sequentially over a set of discrete time points $t = 1, 2, \dots, T$. Specifically, an HMM makes the following set of conditional independence assumptions to model the hidden and the observed processes

$$p(c_t \mid \mathbf{c}_{1:(t-1)}) = p(c_t \mid c_{t-1}), \quad (1)$$

$$p(\mathbf{y}_t \mid \mathbf{y}_{1:(t-1)}, \mathbf{c}_{1:(t-1)}) = p(\mathbf{y}_t \mid c_t). \quad (2)$$

The distributions $p(c_t \mid c_{t-1})$ and $p(\mathbf{y}_t \mid c_t)$ are often referred to as the *transition distribution* and the *emission distribution*, respectively.

A challenging problem of the HMM framework is the determination of the cardinality of the state space. This is rarely exactly known in practice and is often determined using ad hoc model selection approaches. Teh *et al.* (2006) developed a Bayesian nonparametric approach to HMMs based on the hierarchical Dirichlet process (HDP) that defines a prior distribution on transition matrices over a countably infinite number of states. The number of latent states for any given dataset can be inferred from its posterior, allowing for uncertainty in the analysis and also the possibility that additional states may be required when more data points become available, precluding the necessity to decide *a priori* the size of the state space.

One serious limitation of the HDP-HMM in particular and the basic HMM framework in general is the restrictive assumption of first order Markovian dynamics of the latent sequence $\{c_t\}$. The focus of this article is on higher order HMMs (HOHMMs) that extend the idea of basic HMMs by allowing the latent sequence $\{c_t\}$ to depend on its more distant past. An HOHMM of maximal order q thus makes the following set of conditional independence assumptions

$$p(c_t \mid \mathbf{c}_{1:(t-1)}) = p(c_t \mid \mathbf{c}_{(t-q):(t-1)}), \quad (3)$$

$$p(\mathbf{y}_t \mid \mathbf{y}_{1:(t-1)}, \mathbf{c}_{1:(t-1)}) = p(\mathbf{y}_t \mid c_t). \quad (4)$$

We distinguish between an HOHMM of *maximal order* q and an HOHMM of *full order* q . An HOHMM is said to be of maximal order q if conditional on the values

of c_{t-1}, \dots, c_{t-q} , the distribution of c_t is independent of its more distant past, but the lags actually important in determining the distribution of c_t may be an arbitrary subset of $\{c_{t-1}, \dots, c_{t-q}\}$. In contrast, if the distribution of c_t actually varies with the values at all the previous q times points, we call the HOHMM to be of full order q . The case $q = 0$ corresponds to serial independence of the observation sequence $\{\mathbf{y}_t\}$. Also, we say that an HOHMM of maximal order q has *true* maximal order q , if the set of important predictors of c_t includes c_{t-q} .

While the HOHMM framework relaxes the restrictive first order assumption of the basic HMM, it also brings in a daunting dimensionality challenge. Consider, for instance, an HOHMM with C states and maximal order q . The transition distributions are now indexed by the C^q different possible values of the lags $\mathbf{c}_{(t-q):(t-1)}$ (rather than just c_{t-1}), and involve a total number of $(C - 1)C^q$ parameters, which increases exponentially with the order and becomes too large to be estimated efficiently with datasets of the sizes typically encountered in practice. The issue is further complicated by the fact that we do not directly observe the values of the latent sequence $\{c_t\}$ but only their noisy manifestations $\{\mathbf{y}_t\}$. Parsimonious characterization of the transition dynamics is thus extremely important. It is also important to obtain an interpretable structure, with unnecessary lags eliminated.

These daunting challenges to higher order generalizations have forced researchers to focus on the basic HMM, contributing to the immense popularity of the latter and the rarity of the literature on the former. Thede and Harper (1999) used a second order HMM for parts of speech tagging, estimating the transition probabilities by weighted mixtures of empirical proportions of subsequences of maximal length three. Seifert *et al.* (2012) developed an HOHMM with known finite state space and Normal emission densities for modeling array comparative genomic hybridization (aCGH) data. Transition dynamics of maximal order q were modeled using state context trees of maximal depth q that divide the set of all possible state combination histories into disjoint sets of equivalent state contexts. Tree-based strategies employ strict top-down search for important lags and hence are not suitable for scenarios when distant lags may be more important than recent ones (Jääskinen *et al.*, 2014; Sarkar and Dunson, 2016).

In this article, we develop a novel Bayesian nonparametric approach to HOHMMs that can parsimoniously characterize the transition dynamics of any HOHMM with a specified maximal order, allows flexibility in modeling the emission distributions, admits generalizations to countably infinite state spaces, precluding the necessity to predetermine the number of states, and allows automated selection of the important lags, determining the true order and nature of the serial dependence, removing the necessity to decide *a-priori* the exact order of the transition dynamics as well.

We begin by structuring the transition probabilities $p(c_t \mid \mathbf{c}_{(t-q):(t-1)})$ as a high dimensional conditional probability tensor. Adapting the conditional tensor factoriza-

tion approach of Yang and Dunson (2016) to the HOHMM setting, we parameterize the probabilities $p(c_t | \mathbf{c}_{(t-q):(t-1)})$ as mixtures of ‘core’ probability kernels with mixture weights depending on the state combinations of the lags. Such a parameterization explicitly identifies the set of important lags and implicitly captures complex higher order interactions among the important lags, borrowing strength across the states of the HOHMM by sharing the core kernels in a ‘soft’ probabilistic manner. The elimination of the redundant lags and the implicit modeling of the interactions among the important ones can lead to a significant two fold reduction in the effective number parameters required to flexibly characterize the transition dynamics of the HOHMM. We assign sparsity inducing priors that favor such lower dimensional representations of the transition probability tensor.

We assign a hierarchical Dirichlet prior on the core probability kernels, encouraging the model to shrink further towards lower dimensional structures by borrowing strength across these components as well. This also facilitates a generalization to countably infinite state space HOHMMs that precludes the necessity to predetermine the number of states. The HDP-HMM of Teh *et al.* (2006) corresponds to a special case when the kernel sharing feature is turned off and the order is restricted to one.

We develop an efficient two-stage Markov chain Monte Carlo (MCMC) algorithm for learning the parameters of the model. The first stage selects the important lags implementing a coarser ‘hard’ sharing approximation using a stochastic search variable selection (SSVS) approach (George and McCulloch, 1997). The second stage keeps the set of important lags fixed and implements the finer soft kernel sharing feature, building on existing computational machineries for the HDP-HMM.

HOSVD-type factorizations have previously been employed in Sarkar and Dunson (2016) to model the transition dynamics of observable state sequences in a higher order Markov chain framework. The framework of HOHMM, however, brings in significant additional challenges. Unlike an observable Markov process, the states c_t are now latent, only their noisy manifestations \mathbf{y}_t are available. The size of the state space is rarely known and has to be inferred from these noisy data points. These issues make infinite state space models particularly relevant in the HOHMM context. The emission distributions $p(\mathbf{y}_t | c_t)$ have to be additionally modeled which brings in identifiability issues and computational challenges.

The rest of the article is organized as follows. Section 2 details the proposed tensor factorization based HOHMMs and their properties. Section 3 describes Markov chain Monte Carlo (MCMC) algorithms for drawing samples from the posterior. Section 4 presents the results of simulation experiments comparing our method with existing approaches. Section 5 presents some real world applications. Section 6 contains concluding remarks.

2 Higher Order Hidden Markov Model

2.1 Modeling the Transition Probabilities

We build on the idea of higher order singular value decomposition (HOSVD) tensor factorization to develop a nonparametric approach for modeling the transition dynamics of a finite memory HOHMM. HOSVD (Tucker, 1966; De Lathauwer *et al.*, 2000) factorizes a $C_1 \times \dots \times C_p$ dimensional p -way tensor $\mathbf{M} = \{m_{x_1, \dots, x_p}\}$ as

$$m_{x_1, \dots, x_p} = \sum_{h_1=1}^{k_1} \dots \sum_{h_p=1}^{k_p} g_{h_1, \dots, h_p} \prod_{j=1}^p u_{h_j x_j}^{(j)},$$

where the *core tensor* $\mathbf{G} = \{g_{h_1, \dots, h_p}\}$ captures the interactions between different components and $\mathbf{U}^{(j)} = \{u_{h_j x_j}^{(j)}\}$ are component specific weights.

In our HOHMM setting, the hidden sequence $\{c_t\}$ with known state space $\{1, \dots, C\}$ has finite memory of true maximal order q . Given c_{t-q}, \dots, c_{t-1} , the distribution of c_t is thus independent of all latent states prior to $t-q$. The variables that are important in predicting c_t comprise a subset of $\{c_{t-q}, \dots, c_{t-1}\}$, possibly proper but including c_{t-q} .

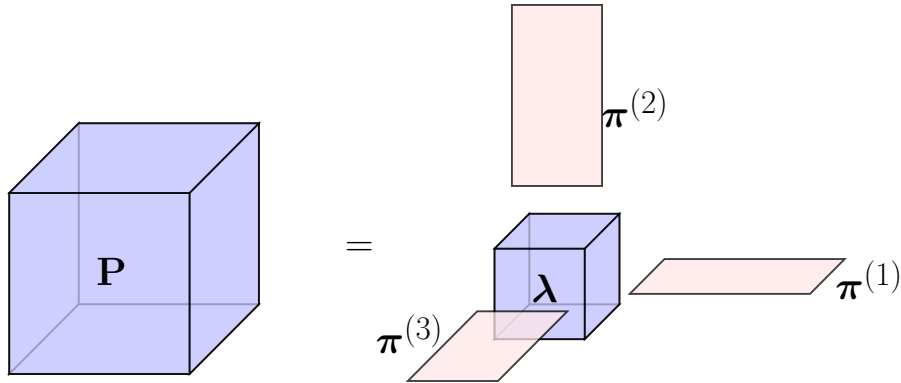


Figure 1: Pictorial representation of the factorization of a transition probability tensor \mathbf{P} characterizing a Markov chain of maximal order 3 with core tensor $\boldsymbol{\lambda}$ and mode matrices $\boldsymbol{\pi}^{(j)}$, $j = 1, 2, 3$.

We structure the transition probabilities $p(c_t | c_{t-q}, \dots, c_{t-1})$ as a $C \times C \times \dots \times C$ dimensional $(q+1)$ -way tensor and consider the following HOSVD-type factorization

$$p(c_t | c_{t-j}, j = 1, \dots, q) = \sum_{h_1=1}^{k_1} \dots \sum_{h_q=1}^{k_q} \lambda_{h_1, \dots, h_q}(c_t) \prod_{j=1}^q \pi_{h_j}^{(j)}(c_{t-j}). \quad (5)$$

See Figure 1. Here $1 \leq k_j \leq C$ for all j and the parameters $\lambda_{h_1, \dots, h_q}(c_t)$ and $\pi_{h_j}^{(j)}(c_{t-j})$ are all non-negative and satisfy the constraints (a) $\sum_{c_t=1}^C \lambda_{h_1, \dots, h_q}(c_t) = 1$, for each combination (h_1, \dots, h_q) , and (b) $\sum_{h_j=1}^{k_j} \pi_{h_j}^{(j)}(c_{t-j}) = 1$, for each pair (j, c_{t-j}) . It follows as a direct consequence of a more general result on conditional probability tensors in Yang and Dunson (2016) that any transition probability tensor can be represented as (5) with the parameters satisfying the constraints (a) and (b).

Introducing latent allocation variables $z_{j,t}$ for $j = 1, \dots, q$ and $t = q + 1, \dots, T$, the latent variables $\{c_t\}$ are conditionally independent and the factorization can be equivalently represented through the following hierarchical formulation

$$(c_t \mid z_{j,t} = h_j, j = 1, \dots, q) \sim \text{Mult}(\{1, \dots, C\}, \lambda_{h_1, \dots, h_q}(1), \dots, \lambda_{h_1, \dots, h_q}(C)), \quad (6)$$

$$(z_{j,t} \mid c_{t-j}) \sim \text{Mult}(\{1, \dots, k_j\}, \pi_1^{(j)}(c_{t-j}), \dots, \pi_{k_j}^{(j)}(c_{t-j})). \quad (7)$$

See Figure 2. Equation (7) reveals the soft sharing property of the model that enables it to borrow strength across the different states of c_{t-j} by allowing the $z_{j,t}$'s associated with a particular state of c_{t-j} to be allocated to different latent populations, which are shared across all C states of c_{t-j} . In contrast, a hard sharing model would allocate each $z_{j,t}$ to some latent population with probability one, still allowing sharing of information across different states but in a coarser fashion. Equation (6) shows how such soft assignment enables the model to capture complex interactions among the lags in an implicit and parsimonious manner by allowing the latent populations indexed by (h_1, \dots, h_q) to be shared among the various state combinations of the lags.

When $k_j = 1$, $\pi_1^{(j)}(c_{t-j}) = 1$ and $P(c_t \mid c_{t-q}, \dots, c_{t-1})$ does not vary with c_{t-j} . The variable k_j thus determines the inclusion of the j^{th} lag c_{t-j} in the model. The variable k_j also determines the number of latent classes for the j^{th} lag c_{t-j} . The number of parameters in such a factorization is given by $(C - 1) \prod_{j=1}^q k_j + C \sum_{j=1}^q (k_j - 1)$, which will be much smaller than the number of parameters $(C - 1)C^q$ required to specify a full Markov model of the same maximal order, if $\prod_{j=1}^q k_j \ll C^q$.

In practical applications, the estimation of $\prod_{j=1}^q k_j$ independent parameters may still be a daunting task. Towards a more parsimonious representation of the transition probability tensor, we assign a hierarchical Dirichlet prior on $\boldsymbol{\lambda}_{h_1, \dots, h_q} = \{\lambda_{h_1, \dots, h_q}(1), \dots, \lambda_{h_1, \dots, h_q}(C)\}$. Specifically, we let

$$\boldsymbol{\lambda}_{h_1, \dots, h_q} \sim \text{Dir}\{\alpha \lambda_0(1), \dots, \alpha \lambda_0(C)\}, \text{ independently for each } (h_1, \dots, h_q), \quad (8)$$

$$\boldsymbol{\lambda}_0 = \{\lambda_0(1), \dots, \lambda_0(C)\} \sim \text{Dir}(\alpha_0/C, \dots, \alpha_0/C). \quad (9)$$

The ‘kernels’ $\boldsymbol{\lambda}_{h_1, \dots, h_q}$ are associated with the mixture weights in a hierarchical DP.

The dimension of $\boldsymbol{\pi}_{k_j}^{(j)}(c_{t-j}) = \{\pi_1^{(j)}(c_{t-j}), \dots, \pi_{k_j}^{(j)}(c_{t-j})\}$, unlike the $\boldsymbol{\lambda}_{h_1, \dots, h_q}$'s,

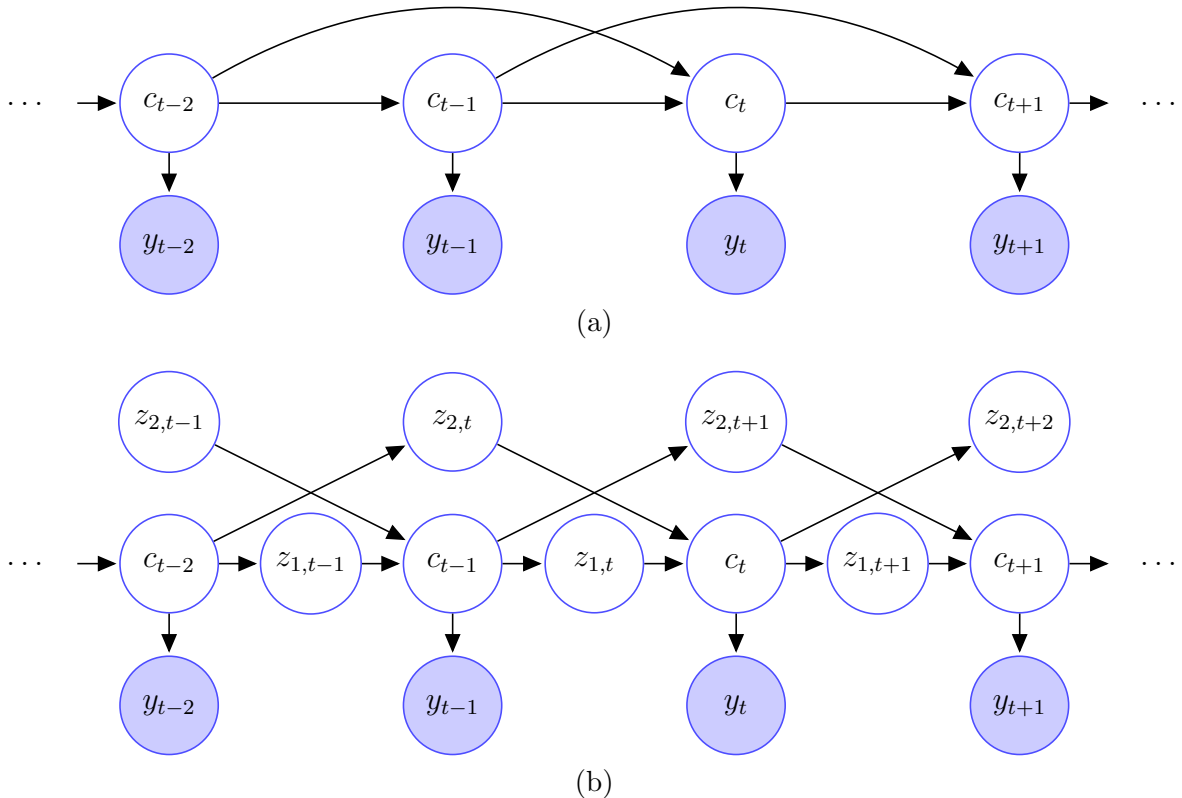


Figure 2: Graphical model depicting the dependence structure of a second order hidden Markov model (a) without and (b) with second level latent variables. Shaded and unshaded nodes represent observed and latent variables, respectively.

varies only linearly with k_j . We assign independent priors on the $\boldsymbol{\pi}_{k_j}^{(j)}(c_{t-j})$'s as

$$\boldsymbol{\pi}_{k_j}^{(j)}(c_{t-j}) = \{\pi_1^{(j)}(c_{t-j}), \dots, \pi_{k_j}^{(j)}(c_{t-j})\} \sim \text{Dir}(\gamma_j, \dots, \gamma_j),$$

independently for each pair (j, c_{t-j}) . (10)

While the dimension of the core tensor varies with k_j 's, all $\boldsymbol{\lambda}_{h_1, \dots, h_q}$ share the same support $\{1, \dots, C\}$. This allows us to avoid conditioning on the k_j 's while specifying the hierarchical prior on $\boldsymbol{\lambda}_{h_1, \dots, h_q}$. The probability vectors $\boldsymbol{\pi}_{k_j}^{(j)}(c_{t-j})$, on the other hand, are supported on $\{1, \dots, k_j\}$ for each pair (j, c_{t-j}) . Therefore, unlike $\boldsymbol{\lambda}_{h_1, \dots, h_q}$, conditioning on k_j , which we have kept implicit in (10), can not be avoided.

Finally, we assign the following independent priors on k_j 's

$$p_{0,j}(k) \propto \exp(-\varphi j k), \quad j = 1, \dots, q, \quad k = k_{j,\min}, \dots, C, \quad (11)$$

where $\varphi > 0$, $k_{j,\min} = 1, j = 1, \dots, q - 1$ and $k_{q,\min} = 2$. The prior $p_{0,j}$ assigns increasing probabilities to smaller values of k_j as the lag j becomes more distant,

reflecting the natural belief that increasing lags have diminishing influence on the distribution of c_t . The larger the value of φ , the faster is the decay of $p_{0,j}(k)$ with increase in j and k , favoring sparser lower order models. The restriction $k_q > 1$ implies that the q^{th} lag is important so that the true maximal order is q .

2.2 Modeling the Emission Distribution

The generic form of the emission distribution that we consider in this article is

$$p(\mathbf{y}_t \mid c_t, \boldsymbol{\theta}, \boldsymbol{\psi}) = f(\mathbf{y}_t \mid \boldsymbol{\theta}_{c_t}, \boldsymbol{\psi}).$$

Here $\boldsymbol{\theta} = \{\boldsymbol{\theta}_c : c = 1, \dots, C\}$ denotes parameters indexed by the latent process $\{c_t\}$, whereas $\boldsymbol{\psi}$ collects global parameters that do not evolve with time but remain constant and may sometimes be kept implicit.

In the first order HMM literature, parametric choices for the emission distribution are common. Leroux (1992) provided sufficient conditions for identifiability in such a framework. Parametric choices for the emission distribution may lead to poor performance, particularly when interest lies in clustering the observed variables according to their latent states. In the HMM literature, this has resulted in recent interest in flexible models for the emission distributions, which can be shown to satisfy sufficient conditions for identifiability (Yau *et al.*, 2011; Fox *et al.*, 2008). Gassiat *et al.* (2015).

The following lemma extends this result to higher order settings. The proof, deferred to S.1, utilizes the fact that any higher order Markov chain $\{c_t\}$ of maximal order q with state space $\mathcal{C} = \{1, \dots, C\}$ and transition probability tensor P can be represented as first order Markov chain $\{\tilde{\mathbf{c}}_t = (c_{t-q+1}, \dots, c_t)\}$ with expanded state space \mathcal{C}^q and transition probability matrix \tilde{P} with entries

$$\begin{aligned} & \tilde{P}\{(j_{t-q}, \dots, j_{t-1}), (i_{t-q+1}, \dots, i_t)\} \\ &= p\{(c_{t-q+1} = i_{t-q+1}, \dots, c_t = i_t) \mid (c_{t-q} = j_{t-q}, \dots, c_{t-1} = j_{t-1})\} \\ &= \begin{cases} P(c_t = i_t \mid c_{t-q} = j_{t-q}, \dots, c_{t-1} = j_{t-1}), & \text{if } i_{t-\ell} = j_{t-\ell} \text{ for } \ell = 1, \dots, (q-1), \\ 0, & \text{otherwise.} \end{cases} \end{aligned}$$

Lemma 1. *Let P be the transition probability tensor and \mathbf{f} be the emission distributions of an HOHMM with known state space \mathcal{C} and known true maximal order q . Let the first order representation of the underlying Markov chain be ergodic and stationary with transition probability matrix \tilde{P} and stationary distribution $\{\pi(c_1, \dots, c_q) : c_j \in \mathcal{C}, j = 1, \dots, q\}$. Let $\boldsymbol{\pi}$ be also the initial distribution of the HOHMM. Let \tilde{P} be of full rank and the emission distributions $\mathbf{f} = \{f_c : c \in \mathcal{C}\}$ be linearly independent as elements of the vector space of signed measures. Then P and \mathbf{f} are nonparametrically identifiable from the distribution of $3q$ consecutive observations*

$\mathbf{y}_{1:3q}$ up to label switching of the states.

Lemma 1 covers a broad class of emission distributions including exponential families and their mixtures, nonparametric discrete distributions, zero inflated Poisson distributions etc. (Gassiat *et al.*, 2015).

Lemma 1 assumes nonsingularity of \tilde{P} . This does not necessarily limit its applicability to HOHMMs of full orders but also accommodates lag gaps. In this case, the transition probability matrix \tilde{P} will have multiple rows sharing the same nonzero elements but they will appear in different columns so that \tilde{P} could still have full rank. Consider, for example, a binary Markov chain of maximal order 2 with a lag gap at $t - 1$, in which case $P(c_t | c_{t-2}, c_{t-1}) = P(c_t | c_{t-2})$ and \tilde{P} is given by

$$\tilde{P} = \begin{array}{cc} & \begin{array}{cccc} (1, 1) & (1, 2) & (2, 1) & (2, 2) \end{array} \\ \begin{array}{c} (1, 1) \\ (1, 2) \\ (2, 1) \\ (2, 2) \end{array} & \left[\begin{array}{cccc} P(1 | 1) & P(2 | 1) & 0 & 0 \\ 0 & 0 & P(1 | 1) & P(2 | 1) \\ P(1 | 2) & P(2 | 2) & 0 & 0 \\ 0 & 0 & P(1 | 2) & P(2 | 2) \end{array} \right]. \end{array}$$

The implication of the restriction $k_q > 1$ in ensuring nonsingularity of \tilde{P} is now clear.

A result on identifiability of HOHMMs in parametric settings can be derived along the lines of Leroux (1992) where only ergodicity of \tilde{P} suffices. For such parametric choices, an unrestricted independent prior on the k_j 's would suffice and the restriction $k_q > 1$ may be dropped. Treating q to be an upper bound on the maximal order, the proposed model can then select the important lags itself, including zeroth order serial independence cases which can be viewed as HOHMMs with $P(c_t | c_{t-q}, \dots, c_{t-1}) = \pi(c_t)$. However, in applications of HOHMMs, some form of serial dependency would generally be expected and we do not pursue the zeroth order cases any further. Practical strategies that allow the assumption of known true maximal order to be relaxed are discussed in Section 2.5.

2.3 Likelihood Factorization

Collecting all potential predictors of c_t in $\mathbf{w}_t = (w_{1,t}, \dots, w_{q,t})^T$ with $w_{j,t} = c_{t-j}$ for $j = 1, \dots, q$ and $t = t^*, \dots, T$, where $t^* = (q + 1)$, the joint distribution of $\mathbf{y} = \{\mathbf{y}_t : t = 1, \dots, T\}$, $\mathbf{c} = \{c_t : t = t^*, \dots, T\}$ and $\mathbf{z} = \{z_{j,t} : t = t^*, \dots, T, j = 1, \dots, q\}$ admits the following factorization

$$p(\mathbf{y}, \mathbf{c}, \mathbf{z} | \boldsymbol{\lambda}_{\mathbf{k}}, \boldsymbol{\pi}_{\mathbf{k}}, \mathbf{k}) = \prod_{t=t^*}^T \left\{ p(c_t | \boldsymbol{\lambda}_{\mathbf{z}_t}) \prod_{j=1}^q p(z_{j,t} | w_{j,t}, \boldsymbol{\pi}_{k_j}^{(j)}, k_j) \right\} \prod_{t=1}^T f(\mathbf{y}_t | \boldsymbol{\theta}_{c_t}, \boldsymbol{\psi})$$

$$\begin{aligned}
&= \prod_{t=1}^T f(\mathbf{y}_t \mid \boldsymbol{\theta}_{c_t}, \boldsymbol{\psi}) \prod_{t=t^*}^T \{p(c_t \mid \boldsymbol{\lambda}_{\mathbf{z}_t}) p(\mathbf{z}_t \mid \mathbf{w}_t, \boldsymbol{\pi}_{\mathbf{k}}, \mathbf{k})\} \\
&= p(\mathbf{y} \mid \mathbf{c}, \boldsymbol{\theta}, \boldsymbol{\psi}) p(\mathbf{c} \mid \mathbf{z}, \boldsymbol{\lambda}_{\mathbf{k}}, \mathbf{k}) \prod_{j=1}^q p(\mathbf{z}_j \mid \mathbf{w}_j, \boldsymbol{\pi}_{k_j}^{(j)}, k_j) \\
&= p(\mathbf{y} \mid \mathbf{c}, \boldsymbol{\theta}, \boldsymbol{\psi}) p(\mathbf{c} \mid \mathbf{z}, \boldsymbol{\lambda}_{\mathbf{k}}, \mathbf{k}) p(\mathbf{z} \mid \mathbf{w}, \boldsymbol{\pi}_{\mathbf{k}}, \mathbf{k}), \tag{12}
\end{aligned}$$

Here $\mathbf{k} = \{k_j : j = 1, \dots, q\}$, $\boldsymbol{\lambda}_{\mathbf{k}} = \{\lambda_{h_1, \dots, h_q}(c) : c = 1, \dots, C, h_j = 1, \dots, k_j, j = 1, \dots, q\}$, $\boldsymbol{\pi}_{k_j}^{(j)}(w_j) = \{\pi_{h_j}^{(j)}(w_j) : h_j = 1, \dots, k_j\}$, $\boldsymbol{\pi}_{k_j}^{(j)} = \{\pi_{k_j}^{(j)}(w_j) : w_j = 1, \dots, C\}$, $\boldsymbol{\pi}_{\mathbf{k}} = \{\boldsymbol{\pi}_{k_j}^{(j)} : j = 1, \dots, q\}$. Also, $\mathbf{z}_t = \{z_{j,t} : j = 1, \dots, q\}$ for all $t = t^*, \dots, T$, $\mathbf{z}_j = \{z_{j,t} : t = t^*, \dots, T\}$ for $j = 1, \dots, q$ and $\mathbf{w}_j = \{w_{j,t} : t = t^*, \dots, T\}$. The subscripts \mathbf{k} and k_j signify that the dimensions of the associated parameters depend on them. In what follows, the subscript \mathbf{k} may sometimes be dropped from $\boldsymbol{\lambda}_{\mathbf{k}}$ to highlight that, unlike $\boldsymbol{\pi}_{\mathbf{k}}$, the support of the core probability vectors comprising $\boldsymbol{\lambda}_{\mathbf{k}}$ does not depend on \mathbf{k} . The conditional independence relationships encoded in the factorization are used in deriving MCMC algorithms to draw samples from the posterior in Section 3.

2.4 Prediction

For a q^{th} order HMM with state space \mathcal{C} , transition probabilities $p(c_t \mid c_{t-q}, \dots, c_{t-1})$ and emission distributions $\{f(y \mid c) : c \in \mathcal{C}\}$, where the state-specific and global emission parameters $\boldsymbol{\theta}$ and $\boldsymbol{\psi}$ are implicitly understood, the r -step ahead density of the HOHMM is given by

$$f_{T+r}(y) = \sum_{c_{T+r}} \sum_{c_{T+r-1}} \cdots \sum_{c_{T+1}} f(y \mid c_{T+r}) p(c_{T+r} \mid \mathbf{c}_{(T+r-q):(T+r-1)}) \cdots p(c_{T+1} \mid \mathbf{c}_{(T+1-q):T}).$$

Assuming stationarity with stationary distribution $\boldsymbol{\pi} = \{\pi(c_{t-q+1}, \dots, c_t) : c_j \in \mathcal{C}, j = t - q + 1, \dots, t\}$, for $r \rightarrow \infty$ we then have

$$\sum_{c_{T+r-q}} \cdots \sum_{c_{T+1}} p(c_{T+r} \mid \mathbf{c}_{(T+r-q):(T+r-1)}) \cdots p(c_{T+1} \mid \mathbf{c}_{(T+1-q):T}) \rightarrow \pi(\mathbf{c}_{(T+r-q+1):(T+r)}).$$

The marginal probabilities of occurrences of individual states $i \in \mathcal{C}$, denoted with slight abuse of notation also by $\pi(i)$, may be obtained from $\boldsymbol{\pi}$ by fixing the last (or any other) element in $\boldsymbol{\pi}$ at i and then summing across the values of the remaining entries. That is, $\pi(i) = \sum_{c_{t-q+1}, \dots, c_{t-1}} \pi(c_{t-q+1}, \dots, c_{t-1}, i)$. Likewise, for any $(i, j) \in \mathcal{C}^2$, we

have $\pi(i, j) = \sum_{c_{t-q+1}, \dots, c_{t-2}} \pi(c_{t-q+1}, \dots, c_{t-2}, i, j)$. This implies, as $r \rightarrow \infty$

$$\begin{aligned} & \sum_{c_{T+r-1}} \cdots \sum_{c_{T+1}} p(c_{T+r} | \mathbf{c}_{(T+r-q):(T+r-1)}) \cdots p(c_{T+1} | \mathbf{c}_{(T+1-q):T}) \\ & \rightarrow \sum_{c_{T+r-1}} \cdots \sum_{c_{T+r-q+1}} \pi(\mathbf{c}_{(T+r-q+1):(T+r)}) = \pi(c_{T+r}). \end{aligned}$$

Hence, we have

$$f_{T+r}(y) \rightarrow \sum_c \pi(c) f(y | c).$$

Next, consider a first order HMM, characterized by the transition probabilities $\{P(j | i) = \pi(i, j)/\pi(j) : i, j \in \mathcal{C}\}$, stationary distribution $\{\pi(i) : i \in \mathcal{C}\}$ and emission distributions $\{f(y | c) : c \in \mathcal{C}\}$. The r -step ahead density then approaches the same limit as $r \rightarrow \infty$. That is, we have

$$f_{T+r}(y) = \sum_{c_{T+r}} \sum_{c_{T+r-1}} \cdots \sum_{c_{T+1}} f(y | c_{T+r}) P(c_{T+r} | c_{T+r-1}) \cdots P(c_{T+1} | c_T) \rightarrow \sum_c \pi(c) f(y | c).$$

As will be seen in Section 4, significant gains in efficiency in estimating several steps ahead predictive densities can be achieved through modeling higher order dynamics when such lags are truly present. As the prediction step is increased, the performances of higher and comparable first order HMMs in estimating the predictive densities, will, however, tend to be similar. In both cases, as r increases, the error in estimating $f_{T+r}(y)$ will also tend to stabilize. Since the predictive densities initially depend on the local dependence on the preceding latent states $\mathbf{c}_{(T+1-q):T}$, the error in estimating these states contribute to the error in estimating the r -step ahead predictive densities. As r increases, however, the true and the estimated predictive densities approach the corresponding stationary distributions which are invariant to $\mathbf{c}_{(T+1-q):T}$ and hence the errors stabilize. See Section 4.

2.5 Unknown Maximal Order and Unknown State Space

For ease of exposition, in Sections 2.1-2.4, we assumed the true maximal order and the true size of the state space to be known. In practical applications, one or both of these quantities are often unknown. In this section, we devise practical strategies to relax these assumptions.

We first relax the assumption of known true maximal order. We do this by letting q to be a known upper bound on the maximal order, and use the following prior on

k_j 's.

$$p(k_1, \dots, k_q) \propto 1 \left\{ \sum_{j=1}^q k_j > q \right\} \prod_{j=1}^q p_{0,j}(k), \quad (13)$$

$$p_{0,j}(k) \propto \exp(-\varphi j k), \quad j = 1, \dots, q, \quad k = 1, \dots, C. \quad (14)$$

The restriction $k_q > 1$ is now replaced by $\sum_{j=1}^q k_j > q$ which ensures that at least one lag is important and the transition matrix corresponding to the true order has full rank. The proposed methodology automatically selects the important lags from the set of potentially important ones.

To relax the assumption of known state space, we look toward Bayesian nonparametric models, like the HDP-HMM, that can accommodate potentially countably infinitely many states in the prior and allow the number of states required to model the data to be sampled and inferred from the posterior, accommodating uncertainty in the analysis. Such models also accommodate the possibility that additional latent states may be required to allow the model to grow in complexity as more data points become available. To this end, the finite state space model for the latent sequence $\{c_t\}$ proposed in Section 2.1 can be naturally extended to

$$(c_t \mid z_{j,t} = h_j, j = 1, \dots, q) \sim \boldsymbol{\lambda}_{h_1, \dots, h_q}, \quad (15)$$

$$\boldsymbol{\lambda}_{h_1, \dots, h_q} \sim \text{DP}(\alpha, \boldsymbol{\lambda}_0), \quad \boldsymbol{\lambda}_0 \sim \text{SB}(\alpha_0), \quad (16)$$

$$(z_{j,t} \mid c_{t-j}) \sim \boldsymbol{\pi}_{k_j}^{(j)}(c_{t-j}), \quad \boldsymbol{\pi}_{k_j}^{(j)}(c_{t-j}) \sim \text{Dir}(\gamma_j, \dots, \gamma_j), \quad (17)$$

$$p(k_1, \dots, k_q) \propto 1 \left\{ \sum_{j=1}^q k_j > q \right\} \prod_{j=1}^q p_{0,j}(k_j), \quad p_{0,j}(k_j) \propto \exp(-\varphi j k_j). \quad (18)$$

Here $h_j = 1, \dots, k_j; k_j = 1, \dots, \infty; j = 1, \dots, q$; $\text{DP}(\alpha, \boldsymbol{\lambda}_0)$ denotes a Dirichlet process prior (Ferguson, 1973) with concentration parameter α and base probability measure $\boldsymbol{\lambda}_0$; and $\boldsymbol{\lambda}_0 \sim \text{SB}(\alpha_0)$ denotes the stick-breaking construction (Sethuraman, 1994) of $\boldsymbol{\lambda}_0 = \{\lambda_0(1), \lambda_0(2), \dots\}$ as

$$\lambda_0(\ell) = v_\ell \prod_{m=1}^{\ell-1} (1 - v_m), \quad v_\ell \sim \text{Beta}(1, \alpha_0), \quad \ell = 1, 2, \dots$$

Equation (16) defines an HDP prior on the probability distributions $\boldsymbol{\lambda}$. In the special case of first order HMM, with $q = 1$, the model reduces to

$$(c_t \mid z_t = h) \sim \boldsymbol{\lambda}_h, \quad (19)$$

$$\boldsymbol{\lambda}_h \sim \text{DP}(\alpha, \boldsymbol{\lambda}_0) \text{ for } h = 1, \dots, k, \quad \boldsymbol{\lambda}_0 \sim \text{SB}(\alpha_0) \quad (20)$$

$$(z_t | c_{t-1}) \sim \boldsymbol{\pi}_k(c_{t-1}), \quad \boldsymbol{\pi}_k(c_{t-1}) \sim \text{Dir}(\gamma_j, \dots, \gamma_j), \quad (21)$$

$$p_0(k) \propto \exp(-\varphi k), \quad k = 2, \dots, \infty. \quad (22)$$

The HDP-HMM of Teh *et al.* (2006) is obtained as a special case if we further let $k = \infty$, and $\pi_h(c) = 1$ if $h = c$ and 0 otherwise for all $h = 1, \dots, \infty$. The proposed model thus generalizes the HDP-HMM in at least two directions. First, it models higher order transition dynamics that can also accommodate lag gaps. Second, even in the special first order setting, the soft allocation feature of the model, as opposed to the hard clustering in HDP-HMMs, enables it to often achieve better levels of data compression, resulting in better estimation and prediction performance.

For large and moderately large values of C , the finite state-space model proposed in Section 2.1 gives a weak limit approximation to the infinite dimensional model in (15)-(18) (Ishwaran and Zarepour, 2002; Teh *et al.*, 2006), providing an excellent practical basis for approximate inference for the latter. In effect, as in the case of maximal order, having a known finite upper bound on the state space size suffices. More precise implementations of the infinite state-space model, via straightforward adaptations of the algorithms developed in Section 3, are thus not pursued here.

3 Posterior Computation

In this article, inference about the proposed HOHMM is based on samples drawn from the posterior using MCMC algorithms. In our proposed HOHMM, the values of k_j 's, being crucial in reducing the model size and acting as lag selection indicators, are of inferential importance. Varying values of k_j 's, however, result in varying dimensional models, posing significant additional computational challenges. Dynamic message passing algorithms, such as the forward-backward sampler, are popular strategies for inference in first order HMMs. See Rabiner (1989) for a review and Scott (2002) for Bayesian MCMC based adaptations. Such algorithms cannot, however, be straightforwardly adapted to the HOHMM setting. It is not clear how message passing strategies can be adapted to include inferences about the k_j 's. Even when the k_j 's are known, when higher order lags are present, computing forward or backward messages would require summing across all possible past histories comprising all possible combinations of values of important lags for each state at each time stamp at each iteration. This involves a prohibitively large number of operations.

We address these challenges by designing an efficient two-stage Gibbs sampling strategy for drawing samples from the posterior. In the first stage, we sample the k_j 's from the posterior of a coarser version of the proposed model. This coarser version is itself fully nonparametric where the k_j 's can still be interpreted as lag selection indicators. In the second stage, we sample from the posterior keeping the k_j 's fixed.

The first stage proceeds as follows. The mixture probabilities are now denoted

Algorithm 1

Updating the Latent State Sequence \mathbf{c} and the Latent Variables \mathbf{z}

- 1: Given the current values \mathbf{c} and \mathbf{z} , propose new values \mathbf{c}^{new} and \mathbf{z}^{new} according to $Q(\mathbf{c}^{new}, \mathbf{z}^{new} \mid \mathbf{c}, \mathbf{z}, \zeta) = Q(\mathbf{c}^{new} \mid \mathbf{z}, \zeta)Q(\mathbf{z}^{new} \mid \mathbf{c}^{new}, \zeta)$, where $Q(\mathbf{c} \mid \mathbf{z}, \zeta) \propto \prod_t \lambda_{\mathbf{z}_t}(c_t)p(\mathbf{y}_t \mid c_t)$ and $Q(\mathbf{z} \mid \mathbf{c}, \zeta) = \prod_{j=1}^q \tilde{\pi}_{z_j, t+j}^{(j)}(c_t)$. Accept the proposed values \mathbf{c}^{new} and \mathbf{z}^{new} with probability

$$\min \left\{ \left[\frac{\prod_t \lambda_{\mathbf{z}_t^{new}}(c_t^{new})}{\prod_t \lambda_{\mathbf{z}_t}(c_t)} \frac{\prod_t \lambda_{\mathbf{z}_t}(c_t)}{\prod_t \lambda_{\mathbf{z}_t}(c_t^{new})} \right]^{1/\mathcal{T}(m)}, 1 \right\},$$

with \mathcal{T}_0 and $\mathcal{T}(m) = \max\{\mathcal{T}_0^{1-m/m_0}, 1\}$ denoting the initial and the current annealing temperature, m the current iteration number and m_0 the iteration number at which the temperature reduces to one.

Updating \mathbf{k} , the Cluster Mappings $\pi_{\mathbf{k}}$ and the Latent Variables \mathbf{z}

- Given the current values of k_j and the current clusters $\mathcal{C} = \{\mathcal{C}_{j,r} : j = 1, \dots, q, r = 1, \dots, k_j\}$, do the following for $j = 1, \dots, q$.
- 2: If $k_j < C$, propose to increase k_j to $(k_j + 1)$. If $k_j > 1$, propose to decrease k_j to $(k_j - 1)$. For $1 < k_j < C$, the moves are proposed with equal probabilities. For $k_j = 1$, the increase move is selected with probability 1. For $k_j = C$, the decrease move is selected with probability 1.
 - 3: If an increase move is proposed, randomly split a cluster of w_j into two clusters. If a decrease move is proposed, randomly merge two clusters of w_j into a single cluster.
 - 4: Accept the proposed moves with acceptance rates based on the approximated marginal likelihood (23) if $\sum_{\ell} k_{\ell} > q$. Set the latent variables \mathbf{z} at the cluster allocation variables determined by the cluster mappings $z_{j,t+j} \sim \tilde{\pi}_{k_j}^{(j)}(c_t)$.

Updating the Mixture Weights $\tilde{\pi}_{\mathbf{k}}$

- 5: The parameters $\tilde{\pi}_{k_j}^{(j)}(w_j)$ are determined by the cluster mappings.

Updating the Transition Distribution Parameters $\lambda_{\mathbf{k}}$ and λ_0

- 6: Sample the parameters $\lambda_{h_1, \dots, h_q}$ and λ_0 as in Algorithm 2.

Updating the Parameters of the Emission Distribution

- 7: Sample the parameters ψ and θ as in Algorithm 2.
-

Algorithm 2

Updating the Latent State Sequence \mathbf{c}

1: Sample the c_t 's from their multinomial full conditionals

$$p(c_t | \zeta) \propto \lambda_{z_1, t, \dots, z_q, t}(c_t) \prod_{j=1}^q \pi_{z_j, t+j}^{(j)}(c_t) f(\mathbf{y}_t | \boldsymbol{\theta}_{c_t}, \boldsymbol{\psi}).$$

Updating the Second Level Latent Variables \mathbf{z}

2: Sample the $z_{j,t}$'s from their multinomial full conditionals

$$p(z_{j,t} = h | \zeta, z_{\ell,t} = h_\ell, \ell \neq j) \propto \pi_h^{(j)}(w_{j,t}) \lambda_{h_1, \dots, h_{j-1}, h, h_{j+1}, \dots, h_q}(c_t).$$

Updating the Mixture Weights $\boldsymbol{\pi}_k$

3: Let $n_{j,w_j}(h_j) = \sum_t 1\{w_{j,t} = w_j, z_{j,t} = h_j\}$. Sample $\boldsymbol{\pi}_{k_j}^{(j)}(w_j)$ as

$$\{\pi_1^{(j)}(w_j), \dots, \pi_{k_j}^{(j)}(w_j)\} | \zeta \sim \text{Dir}\{\gamma_j + n_{j,w_j}(1), \dots, \gamma_j + n_{j,w_j}(k_j)\}.$$

Updating the Transition Distribution Parameters $\boldsymbol{\lambda}_k$ and $\boldsymbol{\lambda}_0$

4: Let $n_{h_1, \dots, h_q}(c) = \sum_t 1\{z_{1,t} = h_1, \dots, z_{q,t} = h_q, c_t = c\}$. Sample the $\boldsymbol{\lambda}_{h_1, \dots, h_q}$'s as

$$\{\lambda_{h_1, \dots, h_q}(1), \dots, \lambda_{h_1, \dots, h_q}(C)\} | \zeta \sim \text{Dir}\{\alpha \lambda_0(1) + n_{h_1, \dots, h_q}(1), \dots, \alpha \lambda_0(C) + n_{h_1, \dots, h_q}(C)\}.$$

5: For $\ell = 1, \dots, n_{h_1, \dots, h_q}(c)$, sample an auxiliary variable x_ℓ as

$$x_\ell | \zeta \sim \text{Bernoulli} \left\{ \frac{\alpha \lambda_0(c)}{\ell - 1 + \alpha \lambda_0(c)} \right\}.$$

Set $m_{h_1, \dots, h_q}(c) = \sum_\ell x_\ell$.

6: Set $m_0(c) = \sum_{(h_1, \dots, h_q)} m_{h_1, \dots, h_q}(c)$. Sample $\boldsymbol{\lambda}_0$ as

$$\{\lambda_0(1), \dots, \lambda_0(C)\} | \zeta \sim \text{Dir}\{\alpha_0/C + m_0(1), \dots, \alpha_0/C + m_0(C)\}.$$

Updating the Parameters of the Emission Distribution

7: Sample the global parameters $\boldsymbol{\psi}$ from their full conditionals

$$p(\boldsymbol{\psi} | \zeta) \propto p_0(\boldsymbol{\psi}) \prod_{t=1}^T f(\mathbf{y}_t | \boldsymbol{\theta}_{c_t}, \boldsymbol{\psi}).$$

8: Sample the cluster specific parameters $\boldsymbol{\theta}$ from their full conditionals

$$p(\boldsymbol{\theta}_c | \zeta) \propto p_0(\boldsymbol{\theta}_c) \prod_{\{t: c_t=c\}} f(\mathbf{y}_t | \boldsymbol{\theta}_c, \boldsymbol{\psi}).$$

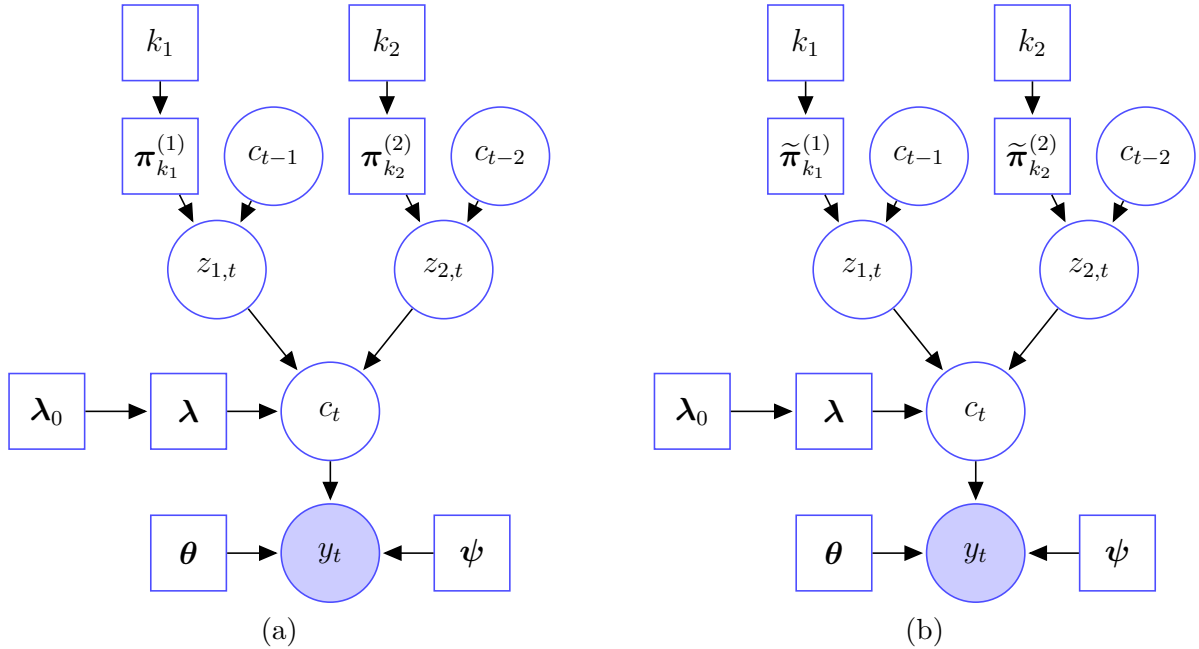


Figure 3: Graphical model depicting the local dependency structure in a second order HMM at time point t . The proposed model (a) and its approximated version (b) that forms the basis of Algorithm 1 described in Section 3. The difference between the two models lies in how the latent variables $z_{j,t}$'s are allocated to different latent clusters. The original model implements a soft clustering of $z_{j,t} \sim \pi_{k_j}^{(j)}(c_{t-j})$ with $\pi_{k_j}^{(j)}(c_{t-j}) \sim \text{Dir}(\gamma_j, \dots, \gamma_j)$ for all j, c_{t-j} . The approximate version implements a hard clustering of $z_{j,t} \sim \tilde{\pi}_{k_j}^{(j)}(c_{t-j})$ with $\tilde{\pi}_{k_j}^{(j)}(c_{t-j}) \in \{0, 1\}$ for all j, h_j and c_{t-j} .

by $\tilde{\pi}_{k_j}$, for reasons to become obvious shortly. Given the current values of \mathbf{k} and \mathbf{c} , we partition the levels of w_j into k_j clusters $\{\mathcal{C}_{j,r} : r = 1, \dots, k_j\}$ with each cluster $\mathcal{C}_{j,r}$ assumed to correspond to its own latent class $h_j = r$. This implies that $\tilde{\pi}_{h_j}^{(j)}(c_{t-j}) = 1$ for some h_j and $\tilde{\pi}_{h_j}^{(j)}(c_{t-j}) = 0$ otherwise, imposing restrictions on soft allocation of the $z_{t,j}$'s, forcing the coarser hard allocation instead. With $\boldsymbol{\lambda}_{h_1, \dots, h_q} \sim \text{Dir}\{\alpha\lambda_0(1), \dots, \alpha\lambda_0(C)\}$ marginalized out, conditional on the cluster configurations $\mathcal{C} = \{\mathcal{C}_{j,r} : j = 1, \dots, q, r = 1, \dots, k_j\}$, we then have

$$p(\mathbf{c} | \mathcal{C}, \boldsymbol{\zeta}) = \prod_{(h_1, \dots, h_q)} \frac{\beta\{\alpha\lambda_0(1) + n_{h_1, \dots, h_q}(1), \dots, \alpha\lambda_0(C) + n_{h_1, \dots, h_q}(C)\}}{\beta\{\alpha\lambda_0(1), \dots, \alpha\lambda_0(C)\}}, \quad (23)$$

where $n_{h_1, \dots, h_q}(c) = \sum_{t=t^*}^T 1\{c_t = c, w_{1,t} \in \mathcal{C}_{1,h_1}, \dots, w_{q,t} \in \mathcal{C}_{m,h_q}\}$. We then use an SSVS approach (George and McCulloch, 1997) based on the approximated marginal likelihood (23) to sample the k_j 's from their posterior. Conditional on \mathbf{k} and the current cluster mappings, we then update \mathbf{c} and \mathbf{z} using a Metropolis-Hastings step. We

chose the proposal distributions that mimic their full conditionals and used simulated annealing to facilitate convergence. See Figure 4 and Algorithm 1 for the second stage described below. The parameters λ , λ_0 , θ and ψ are updated as in the second stage described below.

Conditional on \mathbf{k} , the elements of \mathbf{c} , \mathbf{z} and $\boldsymbol{\pi}$ all have either multinomial or Dirichlet full conditionals and hence can be straightforwardly updated. Conditional on \mathbf{c} and \mathbf{z} , the transition distributions λ and λ_0 can be updated adapting to existing computational machineries for sampling from the posterior in HDP models. The full conditionals of the parameters characterizing the emission distribution depend on the choice of the parametric family used to model the emission distribution but are usually straightforward to compute, often simplified with conjugate priors on the emission parameters. For fixed k_j 's, the parameters of the model can thus be easily sampled from the posterior. One such algorithm for finite state space HOHMM, with the auxiliary variable sampler for HDP (Teh *et al.*, 2006) adapted to our setting, is outlined in Algorithm 2. A Chinese restaurant franchise process analog used to derive this algorithm is presented in the Supplementary Materials.

Additionally, to make the approach even more data adaptive, hyper-priors can be assigned to the prior hyper-parameters α , φ etc. and they can also be sampled from the posterior. Priors and full conditionals used to update these hyper-parameters are outlined in the Supplementary Materials.

Importantly, the finite state space HOHMM provides a weak limit approximation to the infinite state space HOHMM developed in Section 2.5. The two-stage strategy described here may thus also be employed for approximate inference for the infinite state HOHMM.

Specifics of the full conditionals of the emission distribution parameters in steps 7 and 8 of Algorithm 2 naturally depend on the choice of the family and the associated priors. In this article, we consider the following families of emission distributions - (a) Normal, (b) Poisson and (c) translated mixture of Normals.

For Gaussian emission distributions $f(y | c_t = c) = \text{Normal}(y | \mu_c, \sigma_c^2)$. We assigned conjugate $\text{Normal}(\mu_0, \sigma_0^2) \times \text{Inv-Ga}(a_0, b_0)$ prior on (μ_c, σ_c^2) . The posterior full conditional for μ_c and σ_c^2 is then $\text{Normal}(\mu_{c,T}, \sigma_{c,T}^2)$ and $\text{Inv-Ga}\{a_0 + n_c/2, b_0 + \sum_{t:c_t=c} (y_t - \mu_c)^2/2\}$, respectively, where $n_c = \sum_t 1\{c_t = c\}$, $\sigma_{c,T}^{-2} = (\sigma_0^{-2} + n_c\sigma_c^{-2})$ and $\mu_{c,T} = \sigma_{c,T}^{-2}(\mu_0\sigma_0^{-2} + \sum_{t:c_t=c} y_t\sigma_c^{-2})$.

For Poisson emission distributions $f(y | c_t = c) = \text{Poi}(y | \mu_c)$, we assigned conjugate $\text{Ga}(a_0, b_0)$ prior on μ_c , with the hyper-parameters chosen such that $E(\mu_c) = a_0b_0 = \bar{y}$, $\text{var}(\mu_c) = a_0b_0^2 = 2\text{var}(\mathbf{y})$. The posterior full conditional for μ_c is then $\text{Ga}(a_0 + \sum_{t:c_t=c} y_t, b_0 + n_c)$.

Finally, translated mixture Normal emission distributions are constructed as

$$f(y | c_t = c) = \sum_{s=1}^S \pi_s \text{Normal}(y | \mu_c + \eta_s, \sigma_s^2), \quad \text{subject to } \sum_{s=1}^S \pi_s \eta_s = 0.$$

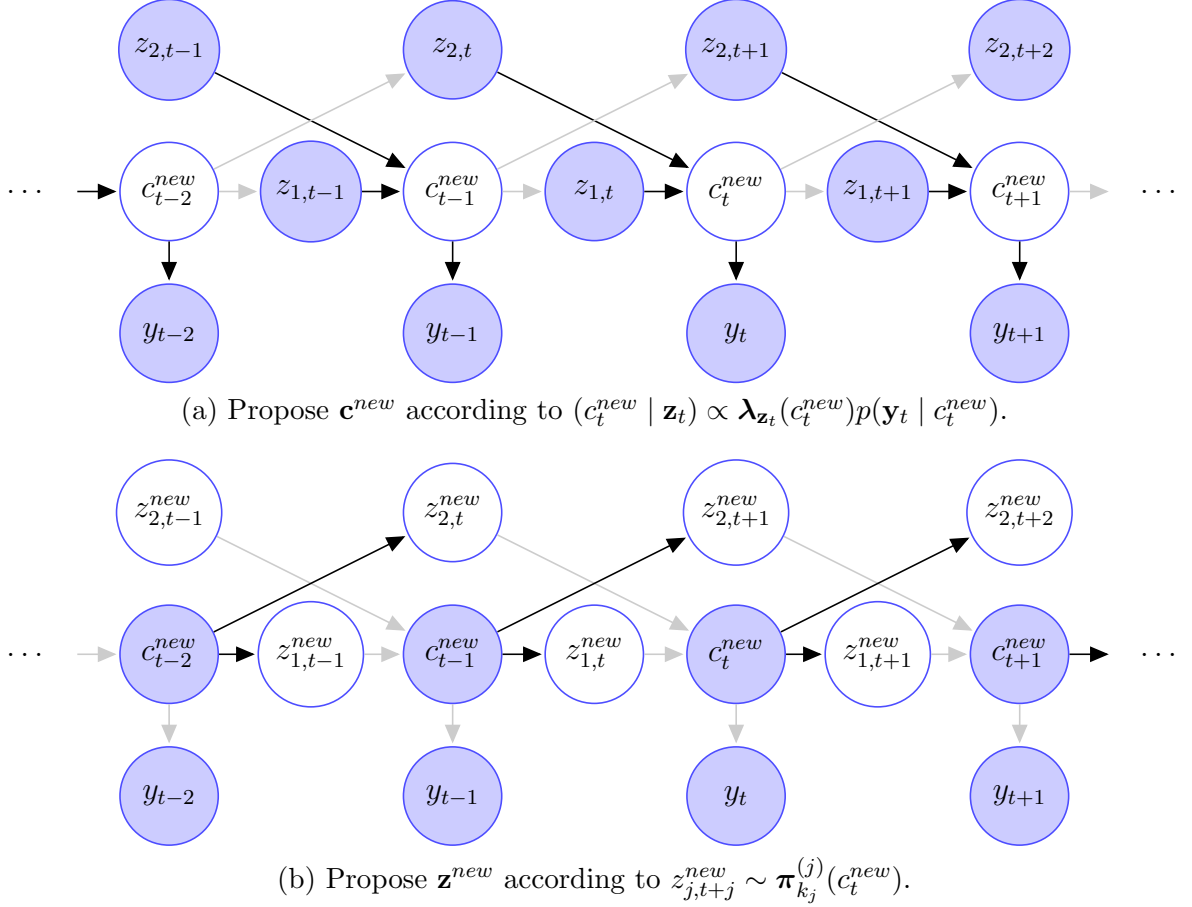


Figure 4: Graphical model showing the mechanisms to propose new values of \mathbf{c} and \mathbf{z} in the Metropolis-Hastings step of the approximate sampler described in Section 3. Starting with Figure 2(b), the lighter edges are ignored in the construction of the proposals.

Introducing additional latent variables $s_t \in \{1, \dots, S\}$ for each t , the model can be rewritten hierarchically as

$$f(y | c_t = c, s_t = s) = \text{Normal}(y | \mu_c + \eta_s, \sigma_s^2), \quad p(s_t = s) = \pi_s.$$

The states s_t 's model local departures from the state specific means μ_c 's but are globally shared across all states. The moment restriction ensures that the marginal mean of each latent state c is still μ_c . The model is similar to that in Yau *et al.* (2011), where they did not have any moment restriction on the globally shared components μ_s but assumed one local mean μ_c to be exactly known to identify the state specific means. We assigned the priors $\mu_c \sim \text{Normal}(\mu_0, \sigma_0^2)$, $\boldsymbol{\pi}_\eta = (\pi_1, \dots, \pi_S)^T \sim \text{Dir}(\alpha_\eta/S, \dots, \alpha_\eta/S)$, $\eta_s \sim \text{Normal}(\mu_{\eta,0}, \sigma_{\eta,0}^2)$, and $\sigma_s^2 \sim \text{Inv-Ga}(a_0, b_0)$. Full condi-

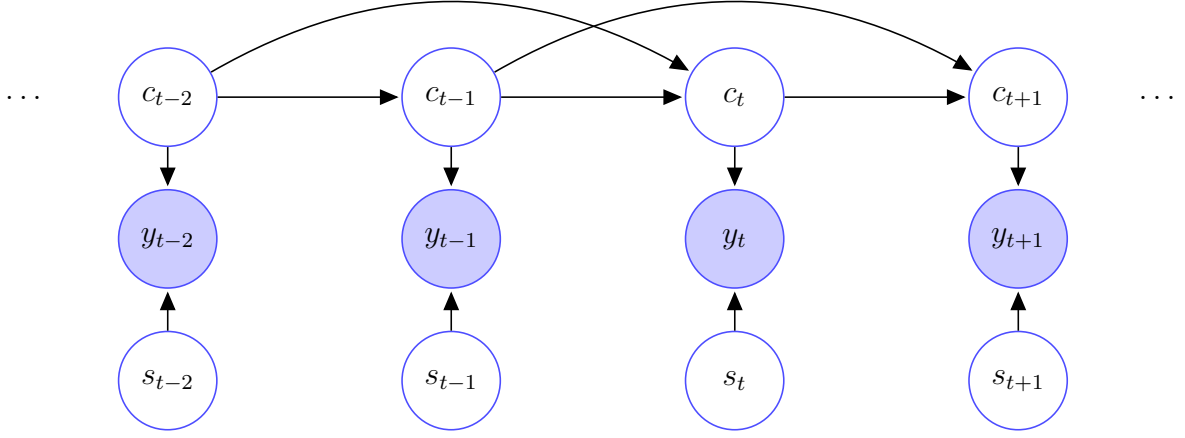


Figure 5: Graphical model depicting the dependence structure of a second order hidden Markov model with translated mixture of Normals as emission distributions.

tionals of μ_c , $\boldsymbol{\pi}_\eta$, σ_s^2 and s_t are then given by

$$\begin{aligned} (\mu_c | \boldsymbol{\zeta}) &\sim \text{Normal}(\mu_{c,T}, \sigma_{c,T}^2), \\ (\sigma_s^2 | \boldsymbol{\zeta}) &\sim \text{Inv-Ga}\{a_0 + n_s/2, b_0 + \sum_{t:s_t=s} (y_t - \mu_{c_t} - \eta_s)^2/2\}, \\ (\boldsymbol{\pi}_\eta | \boldsymbol{\zeta}) &\sim \text{Dir}(\alpha_\eta/S + n_1, \dots, \alpha_\eta/S + n_S), \\ p(s_t = s | \boldsymbol{\zeta}) &\propto \pi_s \times \text{Normal}(y_t | \mu_{c_t} + \eta_s, \sigma_s^2), \end{aligned}$$

where $n_s = \sum_t 1(s_t = s)$, $\sigma_{c,T}^{-2} = (\sigma_0^{-2} + \sum_{t:c_t=c} \sigma_{st}^{-2})$ and $\mu_{c,T} = \sigma_{c,T}^{-2}(\mu_0 \sigma_0^{-2} + \sum_{t:c_t=c} y_t \sigma_{st}^{-2})$. Without the mean restriction, the posterior full conditional of $\boldsymbol{\eta}^{S \times 1} = (\eta_1, \dots, \eta_S)^T$ is given by

$$\text{MVN}_S \left\{ \begin{pmatrix} \eta_1^0 \\ \eta_2^0 \\ \vdots \\ \eta_S^0 \end{pmatrix}, \begin{pmatrix} \sigma_{11}^0 & 0 & \dots & 0 \\ 0 & \sigma_{22}^0 & \dots & 0 \\ \vdots & \vdots & \ddots & \vdots \\ 0 & 0 & \dots & \sigma_{SS}^0 \end{pmatrix} \right\} \equiv \text{MVN}_S(\boldsymbol{\eta}^0, \boldsymbol{\Sigma}^0), \quad (24)$$

where $\sigma_{ss}^0 = (\sigma_{\eta,0}^{-2} + n_s \sigma_s^{-2})^{-1}$, $\eta_s^0 = \sigma_{ss}^0 \{ \sigma_s^{-2} \sum_{t:s_t=s} (y_t - \mu_{c_t}) + \sigma_{\eta,0}^{-2} \mu_{\eta,0} \}$. The posterior full conditional of $\boldsymbol{\eta}$ under the mean restriction can then be obtained easily by further conditioning (24) by $\eta_R = \sum_{s=1}^S \pi_s \eta_s = 0$ and is given by

$$(\boldsymbol{\eta} | \eta_R = 0, \boldsymbol{\zeta}) \sim \text{MVN}_S \{ \boldsymbol{\eta}^0 - \boldsymbol{\sigma}_{1,R}^0 (\boldsymbol{\sigma}_{R,R}^0)^{-1} \eta_R^0, \boldsymbol{\Sigma}^0 - \boldsymbol{\sigma}_{1,R}^0 (\boldsymbol{\sigma}_{R,R}^0)^{-1} \boldsymbol{\sigma}_{R,1}^0 \}, \quad (25)$$

where $\eta_R^0 = \sum_{s=1}^S \pi_s \eta_0 = E(\eta_R)$, $\sigma_{s,S+1} = \pi_s \sigma_{ss}^0 = \text{cov}(\eta_s, \eta_R)$, $\boldsymbol{\sigma}_{R,R}^0 = \sum_{s=1}^S \pi_s^2 \sigma_{ss}^0 = \text{cov}(\eta_R)$, and $\boldsymbol{\sigma}_{R,1}^0 = (\sigma_{1,S+1}, \sigma_{2,S+1}, \dots, \sigma_{S,S+1}) = \boldsymbol{\sigma}_{1,R}^{0T}$. To sample from this singular density, we can first sample from the non-singular distribution of $\{(\eta_1, \eta_2, \dots, \eta_{S-1})^T |$

$\eta_R = 0\}$, which can also be trivially obtained from (25), and then set $\eta_S = -\sum_{s=1}^{S-1} \pi_s \eta_s / \pi_S$.

4 Simulation Experiments

We designed simulation experiments to evaluate the performance of our method in a wide range of scenarios.

For the latent state dynamics, we considered the cases (A) $[3, \{1\}]$, (B) $[3, \{1, 2, 3\}]$, (C) $[3, \{1, 2, 4\}]$, (D) $[3, \{1, 3, 5\}]$, (E) $[3, \{1, 4, 8\}]$, where $[C_0, \{i_1, \dots, i_r\}]$ means that the latent sequence has C_0 categories and $\{c_{t-i_1}, \dots, c_{t-i_r}\}$ are the important lags. In each case, we considered two sample sizes $T = 500, 1000$. To generate the true transition probability tensors, for each combination of the true lags, we first generated the probability of the first response category as $f(u_1) = u_1^2 / \{u_1^2 + (1 - u_1)^2\}$ with $u_1 \sim \text{Unif}(0, 1)$. The probabilities of the remaining categories are then generated via a stick-breaking type construction as $f(u_2)\{1 - f(u_1)\}$ with $u_2 \sim \text{Unif}(0, 1)$ and so on, until the next to last category ($C - 1$) is reached. The hyper-parameters were set at $\alpha_0 = 1$, and $\gamma_j = 1/C$ for all j . In each case, we set the maximal number of states at $C = 10$ and the maximal lag at $q = 10$.

We considered (1) Normal, (2) Poisson and (3) translated mixtures of Normals emission distributions. For the Gaussian case $f(y | c_t = c) = \text{Normal}(y | \mu_c, \sigma_c^2)$, we set $\mu_c = -2, 0, 2$ for $c = 1, 2, 3$, respectively, and $\sigma_c^2 = 0.5^2$ for all c . While the σ_c^2 's were all equal and could be treated as a global parameter, we allowed the component specific variances to be different in the fitted model. The hyper-parameters of the priors were set at $\mu_0 = \bar{\mathbf{y}}, \sigma_0^2 = 3\text{var}(\mathbf{y}), a_0 = b_0 = 1$. For Poisson emission distributions $f(y | c_t = c) = \text{Poi}(y | \mu_c)$, we let $\mu_c = 1, 8, 15$ for $c = 1, 2, 3$, respectively. The hyper-parameters of the Gamma prior on μ_c were chosen such that $E(\mu_c) = a_0 b_0 = \bar{\mathbf{y}}, \text{var}(\mu_c) = a_0 b_0^2 = 2\text{var}(\mathbf{y})$. For translated Gaussian mixture emission distributions $f(y | c_t = c) = \sum_{s=1}^S \pi_s \text{Normal}(y | \mu_c + \eta_s, \sigma_s^2)$, we set $\mu_c = -4, 0, 4$ for $c = 1, 2, 3$; $\pi_s = 0.2, 0.5, 0.3, \eta_s = -2, 0, 1.33$ for $s = 1, 2, 3$; and $\sigma_s^2 = 0.5^2$ for all s . As in the case of simpler Gaussian emissions, even though σ_s^2 's were all equal in the true data generating mechanism, they were allowed to be different in the fitted model.

In each case, we initialized the latent states \mathbf{c} applying a k-means clustering algorithm to \mathbf{y} with $k = C = 5$ states. With $k_1 = 2$ and $k_j = 1$ for $j = 2, \dots, 10$, initially only the first lag was chosen to be important. The parameters $\boldsymbol{\lambda}, \boldsymbol{\lambda}_0, \mathbf{z}, \boldsymbol{\pi}$ etc. were then initialized by randomly sampling from the prior generative model. For Normal emission distributions, (μ_c, σ_c^2) 's were set at the corresponding empirical values; and for Poisson and translated Normal emissions, μ_c 's were set at the corresponding empirical means. For translated Normal emissions, the indices \mathbf{s} and (μ_s, σ_s^2) 's were likewise set using a k-means algorithm applied to $(y_t - \mu_{c_t})$ with $k = S = 5$. In each case, the mean parameters associated with the remaining 5 states were spread

over the range of \mathbf{y} . For Normal emissions, the remaining σ_c^2 's were set at $\text{var}(\mathbf{y})$. In numerical experiments, we found the results to be very robust to the choice of the prior hyper-parameters and parameter and latent variable initializations.

We coded in MATLAB¹. For the case (D1) described above, with $T = 500$ data points, 5,000 MCMC iterations required approximately 30 minutes on an ordinary laptop. In each case, we discarded the first 2000 iterations as burn-in. The remaining samples were thinned by retaining every 5th sample after the burn-in.

| True Dynamics | Sample Size | Median ISE $\times 100$ | | | | | |
|---|-------------|-------------------------|-------|-------|-------------|-------------|-------------|
| | | HDP-HMM | | | CTF-HOHMM | | |
| | | One | Two | Three | One | Two | Three |
| Normal Emission Distribution | | | | | | | |
| (A) 3, {1} | 500 | 0.37 | 0.20 | 0.23 | 0.37 (0.33) | 0.19 (0.17) | 0.20 (0.19) |
| | 1000 | 0.16 | 0.13 | 0.11 | 0.11 (0.11) | 0.11 (0.11) | 0.09 (0.10) |
| (B) 3, {1, 2, 3} | 500 | 10.96 | 8.46 | 4.21 | 0.82 | 0.67 | 0.65 |
| | 1000 | 4.47 | 5.04 | 3.26 | 0.32 | 0.31 | 0.20 |
| (C) 3, {1, 2, 4} | 500 | 11.39 | 8.46 | 6.66 | 0.88 | 0.80 | 0.65 |
| | 1000 | 9.52 | 6.51 | 5.98 | 0.31 | 0.30 | 0.29 |
| (D) 3, {1, 3, 5} | 500 | 10.91 | 11.14 | 9.38 | 0.71 | 0.69 | 0.57 |
| | 1000 | 15.60 | 11.24 | 9.21 | 0.30 | 0.35 | 0.32 |
| Poisson Emission Distribution | | | | | | | |
| (A) 3, {1} | 500 | 0.15 | 0.22 | 0.10 | 0.09 (0.07) | 0.07 (0.05) | 0.05 (0.04) |
| | 1000 | 0.30 | 0.26 | 0.17 | 0.09 (0.04) | 0.05 (0.04) | 0.03 (0.03) |
| (B) 3, {1, 2, 3} | 500 | 3.02 | 1.92 | 1.77 | 1.17 | 0.61 | 0.65 |
| | 1000 | 1.99 | 1.65 | 1.32 | 0.32 | 0.14 | 0.09 |
| (C) 3, {1, 2, 4} | 500 | 2.58 | 1.75 | 1.62 | 0.57 | 0.47 | 0.45 |
| | 1000 | 3.61 | 2.41 | 1.50 | 0.72 | 0.51 | 0.32 |
| (D) 3, {1, 3, 5} | 500 | 4.72 | 1.71 | 2.71 | 2.41 | 1.26 | 0.78 |
| | 1000 | 5.08 | 2.37 | 3.24 | 1.03 | 0.76 | 0.53 |
| Translated Mixture Normal Emission Distribution | | | | | | | |
| (A) 3, {1} | 500 | 0.35 | 0.27 | 0.27 | 0.39 (0.35) | 0.29 (0.29) | 0.27 (0.27) |
| | 1000 | 0.21 | 0.15 | 0.11 | 0.23 (0.22) | 0.20 (0.15) | 0.12 (0.12) |
| (B) 3, {1, 2, 3} | 500 | 5.39 | 3.40 | 2.99 | 1.25 | 1.09 | 0.85 |
| | 1000 | 4.09 | 3.84 | 2.60 | 0.53 | 0.47 | 0.31 |
| (C) 3, {1, 2, 4} | 500 | 6.55 | 3.88 | 3.37 | 1.44 | 1.401 | 1.06 |
| | 1000 | 3.51 | 3.00 | 2.84 | 0.58 | 0.46 | 0.43 |
| (D) 3, {1, 3, 5} | 500 | 7.80 | 5.15 | 2.81 | 3.06 | 1.76 | 1.21 |
| | 1000 | 7.20 | 3.77 | 3.19 | 0.53 | 0.59 | 0.47 |

Table 1: Median ISEs in estimating one two and three step ahead predictive densities for the conditional tensor factorization (CTF) based HOHMM compared with the HDP-HMM. In the first column, $C_0, \{i_1, \dots, i_r\}$ means that the latent sequence truly has C_0 categories and $\{c_{t-i_1}, \dots, c_{t-i_r}\}$ are the true important lags. In the rows corresponding to the first order case (A) 3, {1}, the numbers within parenthesis in the CTF-HOHMM columns show the estimated median MISEs with the maximal order set at $q = 1$. In all other cases, $q = 5$. See Section 4 for additional details.

¹Codes implementing our method will be included as part of the Supplementary Materials once the paper is accepted for publication.

| True Dynamics | Sample | Median Hamming Distance $\times 100$ | |
|---|--------|--------------------------------------|-------------|
| | Size | HDP-HMM | CTF-HOHMM |
| Normal Emission Distribution | | | |
| (A) 3, {1} | 500 | 3.77 | 2.56 (2.23) |
| | 1000 | 2.57 | 2.10 (2.00) |
| (B) 3, {1, 2, 3} | 500 | 19.02 | 2.43 |
| | 1000 | 16.37 | 2.24 |
| (C) 3, {1, 2, 4} | 500 | 20.46 | 2.50 |
| | 1000 | 19.82 | 2.19 |
| (D) 3, {1, 3, 5} | 500 | 16.45 | 2.33 |
| | 1000 | 12.01 | 2.30 |
| Poisson Emission Distribution | | | |
| (A) 3, {1} | 500 | 11.01 | 8.72 (8.10) |
| | 1000 | 12.78 | 8.12 (8.01) |
| (B) 3, {1, 2, 3} | 500 | 23.45 | 12.66 |
| | 1000 | 21.50 | 8.92 |
| (C) 3, {1, 2, 4} | 500 | 23.29 | 10.95 |
| | 1000 | 22.11 | 8.91 |
| (D) 3, {1, 3, 5} | 500 | 21.35 | 14.26 |
| | 1000 | 21.03 | 10.96 |
| Translated Mixture Normal Emission Distribution | | | |
| (A) 3, {1} | 500 | 4.83 | 7.31 (5.80) |
| | 1000 | 4.38 | 6.81 (5.58) |
| (B) 3, {1, 2, 3} | 500 | 19.21 | 7.02 |
| | 1000 | 24.01 | 6.92 |
| (C) 3, {1, 2, 4} | 500 | 17.36 | 10.38 |
| | 1000 | 20.59 | 5.93 |
| (D) 3, {1, 3, 5} | 500 | 14.09 | 15.88 |
| | 1000 | 13.81 | 5.32 |

Table 2: Median Normalized Hamming distances between the true and the estimated state sequences for the conditional tensor factorization (CTF) based HOHMM and the HDP-HMM. In the first column, $C_0, \{i_1, \dots, i_r\}$ means that the latent sequence truly has C_0 categories and $\{c_{t-i_1}, \dots, c_{t-i_r}\}$ are the true important lags. In the rows corresponding to the first order case (A) 3, {1}, the numbers within parenthesis in the CTF-HOHMM columns show the estimated median MISEs with the maximal order set at $q = 1$. In all other cases, $q = 5$. See Section 4 for additional details.

We evaluated the performance of our proposed model and the HDP-HMM in estimating one, two and three-step ahead predictive densities. For an HOHMM of maximal order q , the r -step ahead predictive density is given by

$$\begin{aligned}
f_{T+r}(y|\mathbf{y}) &= E_{P(\boldsymbol{\zeta}, \mathbf{c}|\mathbf{y})} p(y | \mathbf{c}, \boldsymbol{\zeta}) = \int p(y | \mathbf{c}, \boldsymbol{\zeta}) dP(\boldsymbol{\zeta}, \mathbf{c} | \mathbf{y}) \\
&= E_{P(\boldsymbol{\zeta}, \mathbf{c}|\mathbf{y})} \left[\sum_{c_{T+r}} \sum_{c_{T+r-1}} \cdots \sum_{c_{T+1}} f(y | c_{T+r}, \boldsymbol{\zeta}) p(c_{T+r} | \mathbf{c}_{(T+r-q):(T+r-1)}, \boldsymbol{\zeta}) \cdots p(c_{T+1} | \mathbf{c}_{(T+1-q):T}, \boldsymbol{\zeta}) \right].
\end{aligned}$$

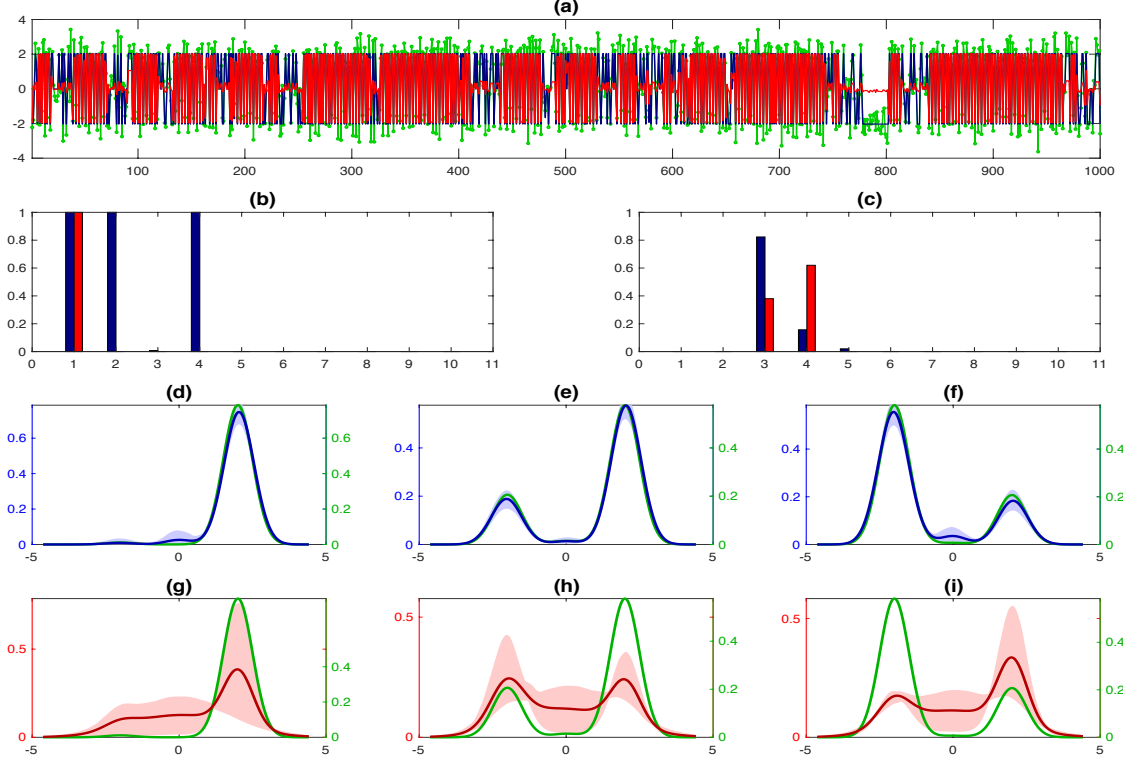


Figure 6: Results for a synthetic dataset in the (D1) case described in Section 4 (transition dynamics $3\{1, 2, 4\}$ and Normal emission densities): CTF-HOHMM in blue and HDP-HMM in red (a) posterior means super-imposed over the observed time series in green; (b) the inclusion probabilities of different lags; (c) the distribution of different number of states; (d), (e), (f) estimated one, two and three steps ahead predictive densities, respectively, and their 90% credible intervals by the CTF-HOHMM; (g), (h), (i) estimated one, two and three steps ahead predictive densities, respectively, and their 90% credible intervals by the HDP-HMM. The true predictive densities are shown in green.

Based on M samples $\{(\mathbf{c}_{1:T}^{(m)}, \zeta^{(m)})\}_{m=1}^M$ drawn from the posterior, $f_{T+r}(y|\mathbf{y})$ can be estimated as

$$\hat{f}_{T+r}(y|\mathbf{y}) = M^{-1} \sum_{m=1}^M \sum_{c_{T+r}} \sum_{c_{T+r-1}} \cdots \sum_{c_{T+1}} f(y | c_{T+r}, \zeta^{(m)}) \\ p(c_{T+r} | \mathbf{c}_{(T+r-q):(T+r-1)}^{(m)}, \zeta^{(m)}) \cdots p(c_{T+1} | \mathbf{c}_{(T+1-q):T}^{(m)}, \zeta^{(m)}),$$

where $\mathbf{c}_{(T+r-q):(T+r-1)}^{(m)} = (c_{T+r-q}^{(m)}, c_{T+r-q+1}^{(m)}, \dots, c_T^{(m)}, c_{T+1}^{(m)}, \dots, c_{T+r-1}^{(m)})$ for all (r, m) . The corresponding true density is given by

$$f_{T+r,0}(y) = \sum_{c_{T+r,0}} \sum_{c_{T+r-1,0}} \cdots \sum_{c_{T+1,0}} f_0(y | c_{T+r,0})$$

$$p_0(c_{T+r,0} \mid \mathbf{c}_{(T+r-q):(T+r-1),0}) \dots p_0(c_{T+1,0} \mid \mathbf{c}_{(T+1-q):T,0}),$$

where p_0 and f_0 are generics for the true transition and emission distributions, respectively, with associated true parameters implicitly understood and $\mathbf{c}_0 = \mathbf{c}_{1:T,0}$ denoting the true values of the latent sequence \mathbf{c} . For continuous emission distributions, the integrated squared error (ISE) in estimating $f_{T+r,0}(y)$ is estimated by $\sum_{i=1}^N \{f_{T+r,0}(y_i^\Delta) - \hat{f}_{T+r}(y_i^\Delta \mid \mathbf{y})\}^2 \Delta_i$, where $\{y_i^\Delta\}_{i=0}^N$ are a set of grid points on the range of y and $\Delta_i = (y_i^\Delta - y_{i-1}^\Delta)$ for all i . For Poisson emission distribution, the ISE is estimated as $\sum_{i=\max\{0, \min \mathbf{y}-1\}}^{\max \mathbf{y}+1} \{f_{T+r,0}(i) - \hat{f}_{T+r}(i \mid \mathbf{y})\}^2$.

We also evaluated the Hamming distance between the true and the estimated state sequences by the proposed HOHMM and the HDP-HMM. To calculate the Hamming distance, we used the Munkres algorithm (Munkres, 1957), mapping the indices of the estimated state sequence to the set of indices that maximize the overlap with the true sequence.

The performances in estimating the one, two and three step ahead predictive densities and in clustering the observations y_t are summarized in Tables 1 and 2, respectively. The reported results are based on 100 simulated datasets in each case. The proposed approach vastly outperformed the HDP-HMM in the higher order cases and remarkably also in the first order parametric cases. Figure 6 summarizes the results for the data set corresponding to the median ISE in estimating the one-step ahead predictive density for the HOHMM in the (D1) case with $T = 1000$. Panel (a) in Figure 6 suggests that the CTF-HOHMM provides a better fit to local variations in the dataset. The improvements in higher order cases are explained by the HDP-HMM's restrictive first order assumption. The proposed method, on the other hand, not just accommodates higher order lags, but also effectively eliminates the unnecessary ones, while also characterizing the dynamics using efficient sparse representations. The improvements in the first order cases can then be attributed to this ability to effectively eliminate the unnecessary lags in correctly identifying the true first order dynamics and then sparsely characterizing that dynamics using better compression models. The remarkable efficiency of the proposed HOHMM method even when the maximal lag is set at large conservative values is also seen from comparisons of the results when the maximal lag was set at 10 with the results reported in parentheses in Tables 1 and 2 that were produced by its first order restriction by prefixing the maximal lag at one. See Figure 7 that summarizes the results for the data set corresponding to the median ISE for the one-step ahead predictive density in the (A3) case with $T = 1000$. Table 1 shows that with increase in the prediction step the performance in estimating the predictive density improved for both the HDP-HMM and the proposed HOHMM. As discussed in Section 2.4, the predictive dynamics initially depend heavily on the latent states $c_{T-i_1+1}, \dots, c_{T-i_r+1}$. The errors in estimating these unknown states thus contribute to the errors in estimating the predictive densities. However, when the

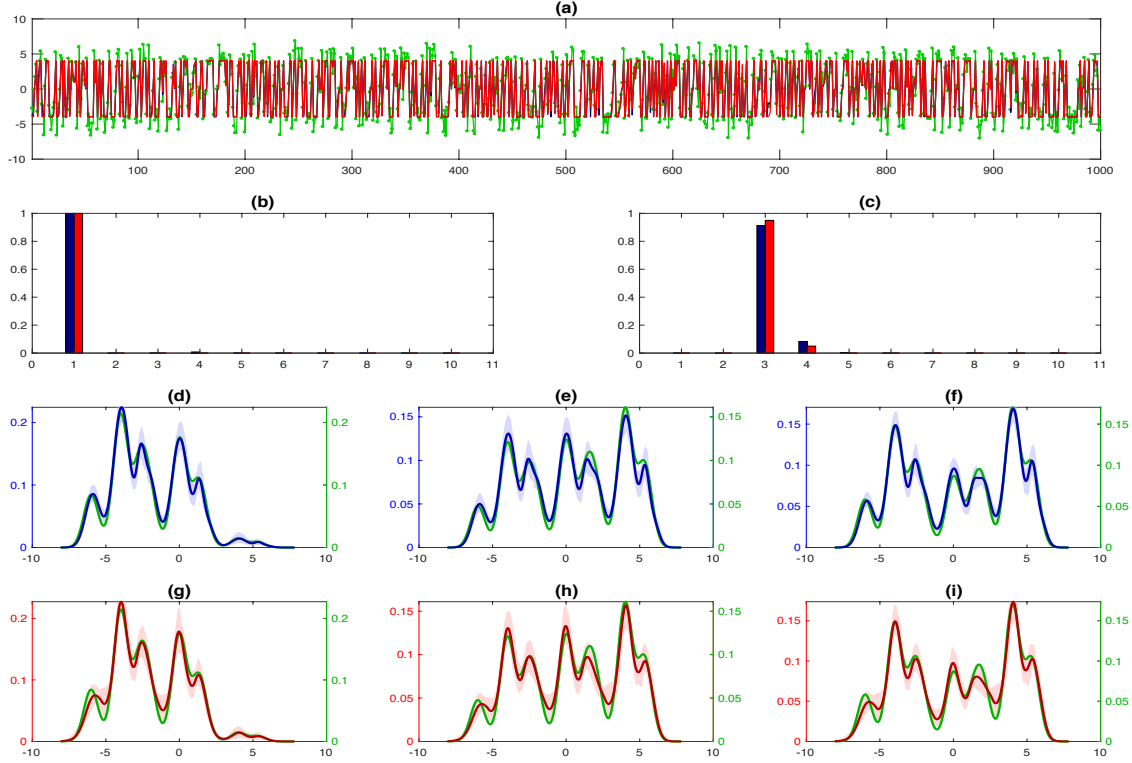


Figure 7: Results for a synthetic dataset in the (A3) case described in Section 4 (transition dynamics $3\{1\}$ and translated Normal emission densities): CTF-HOHMM in blue and HDP-HMM in red (a) posterior means super-imposed over the observed time series in green; (b) the inclusion probabilities of different lags; (c) the distribution of different number of states; (d), (e), (f) estimated one, two and three steps ahead predictive densities, respectively, and their 90% credible intervals by the CTF-HOHMM; (g), (h), (i) estimated one, two and three steps ahead predictive densities, respectively, and their 90% credible intervals by the HDP-HMM. The true predictive densities are shown in green.

prediction step increases, the true and the estimated predictive densities approach the corresponding stationary distributions which are invariant to $c_{T-i_1+1}, \dots, c_{T-i_r+1}$ and the error stabilizes. Improved estimation of the latent states, as evident from the estimated Hamming distances, can likewise be explained by the aforementioned novel aspects of the proposed HOHMM.

5 Applications

In this section, we discuss results of the proposed CTF-HOHMM applied to a few real datasets. The datasets discussed here are all available publicly from various sources. In each case, we compare the results with that produced by the HDP-HMM. Unless otherwise mentioned, each model is allowed a maximum of $C = 10$ states; the HOHMM was allowed a maximal lag of $q = 10$; and the model parameters were all

initialized as in the simulation experiments.

Old Faithful Geyser Data: We first consider the Geyser dataset, accompanying McDonald and Zuchhini (1997) and also available from the MASS package in R. The dataset comprises 299 sequential observations on eruption and waiting times (in minutes) of the Old Faithful geyser in Yellowstone National Park in the USA collected continually from August 1 to August 15, 1985. We focus here on modeling duration times using HMMs with Normal emission distributions. Empirical explorations of the dataset earlier in Section 3 in Azzalini and Bowman (1990) had suggested second order dynamics.

Figure 8 summarizes the results. Results produced by HDP-HMM and CTF-HOHMM are in general agreement, both models suggesting a three state dynamics. The results returned by HOHMM, however, suggest a second order HMM to provide the best fit, consistent with Azzalini and Bowman (1990).

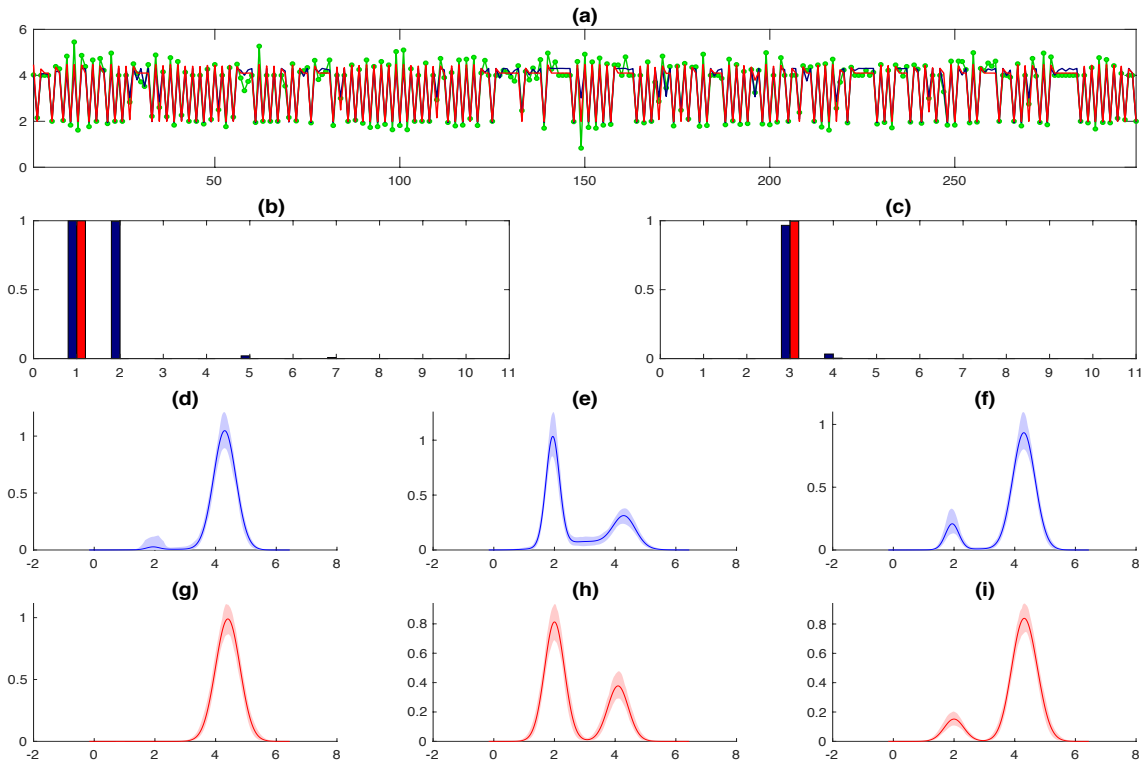


Figure 8: Results for the Geyser dataset: CTF-HOHMM in blue and HDP-HMM in red (a) posterior means super-imposed over the observed time series in green; (b) the inclusion probabilities of different lags; (c) the distribution of different number of states; (d), (e), (f) estimated one, two and three steps ahead predictive densities, respectively, and their 90% credible intervals by the CTF-HOHMM; (g), (h), (i) estimated one, two and three steps ahead predictive densities, respectively, and their 90% credible intervals by the HDP-HMM.

MIT Heart Data: Next, we consider MIT heart data, a collection of 4 time

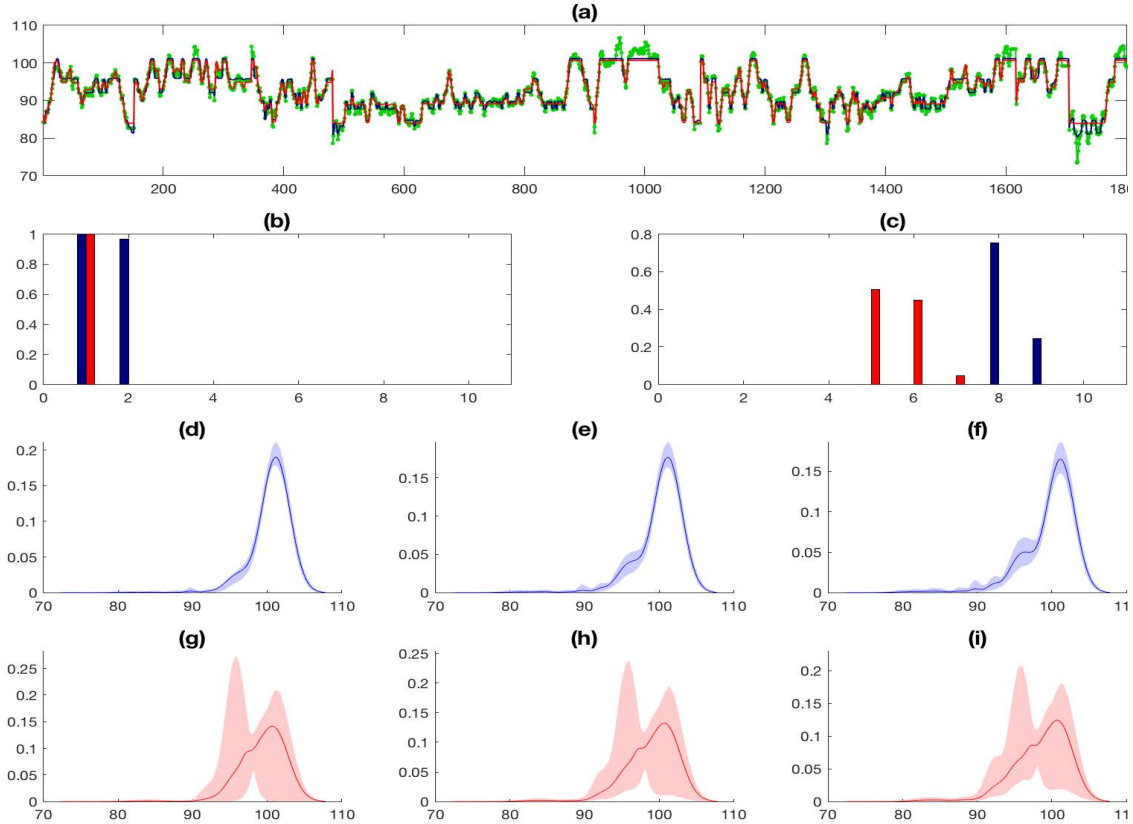


Figure 9: Results for the MIT heart dataset: CTF-HOHMM in blue and HDP-HMM in red (a) posterior means super-imposed over the observed time series in green; (b) the inclusion probabilities of different lags; (c) the distribution of different number of states; (d), (e), (f) estimated one, two and three steps ahead predictive densities, respectively, and their 90% credible intervals by the CTF-HOHMM; (g), (h), (i) estimated one, two and three steps ahead predictive densities, respectively, and their 90% credible intervals by the HDP-HMM.

series. The first two series contains 1800 evenly-spaced measurements of instantaneous heart rate from different subjects performing similar activities. The measurements (in units of beats per minute) occur at 0.5 second intervals over a 15 minute interval.

Figure 9 summarizes the results for the series 1 dataset obtained by the CTF-HOHMM and the HDP-HMM with Normal emission distributions. The HDP-HMM results show uncertainty around the number of underlying latent states, suggesting a mixture of 5 and 6 latent states. The CTF-HOHMM results suggest second order dependencies. Like the HDP-HMM, CTF-HOHMM also accommodates uncertainty in the number of states, suggesting however a mixture of 8 and 9 states. Panel (a) in Figure 9 suggests that the CTF-HOHMM provides a better fit to local variations in the dataset. The predictive densities estimated by the two methods also look substantially different.

The series 2 in the MIT heart dataset shows strong signs of irregular periodicity. HMMs are not suitable for modeling periodicity without additional modifications. We have thus not pursued modeling series 2. The series 3 and 4 were recorded in the same way but contain 950 measurements each, corresponding to 7 minutes and 55 seconds of data in each case. CTF-HOHMM applied to these two datasets suggests first order dependencies in both cases. Results produced by HDP-HMM and CTF-HOHMM, not presented here, were very similar for these two series.

E.coli Data: Next, we consider the E.coli data set available from `tscount` package in R. This dataset comprises weekly number of reported disease cases caused by Escherichia coli in the state of North RhineWestphalia (Germany) from January 2001 to May 2013.

Figure 10 summarizes the results obtained by the CTF-HOHMM and the HDP-HMM with Poisson emission distributions. The HDP-HMM results suggests 5 latent states. The CTF-HOHMM results suggests a first order dynamics but 7 latent states. Panel (a) in Figure 10 suggests that the CTF-HOHMM provides a better fit to local variations in the data. The one, two and three steps ahead predictive densities, however, look similar.

Coriell aCGH Data: Array comparative genomic hybridization (aCGH) studies are used to investigate the identification of DNA polymorphisms - deletions or sequences deviations, or duplications. The measurement at the t^{th} location on the chromosome typically represents \log_2 ratio of copy numbers in the test genome to that in a reference genome. A zero value thus indicates the same copy number as that in the reference genome, positive values indicate gains or amplifications, whereas negative observations represent deletions.

First and higher order HMMs have been used in the literature for modeling aCGH data. Fridlyand *et al.* (2004) used a first order HMM to segment aCGH data into sets with the same underlying copy number; Guha *et al.* (2008b) used a first order HMM with four latent copy number states with Gaussian emission densities; Seifert *et al.* (2012) used a tree based higher order HMM with three states with Gaussian emission densities; Yau *et al.* (2011) used a first order HMM with three states but a flexible infinite component translated-mixture of Normals as the emission distribution. The use of a flexible family of emission densities made this approach robust to the presence of outliers, skewness or heavy tails in the error process.

We consider the Coriell aCGH dataset from the `DNACopy` package in `Bioconductor`, originally presented in Snijders *et al.* (2001). The data correspond to two array CGH studies of fibroblast cell strains. We chose the study GM05296 that comprised copy number ratios at 2271 consecutive genomic locations. We model the dataset using HDP-HMM and the proposed HOHMM with $C = 3$ states. The unknown state specific means μ_c 's are allowed to vary according to $\text{Normal}(\mu_{c,0}, \sigma_{c,0}^2)$ hyper-priors with $\mu_{c,0} = -0.5, 0.0, 0.5$ and $\sigma_{c,0} = 1/6, 10^{-5}, 1/6$ for $c = 1, 2, 3$, allowing μ_c 's to vary over

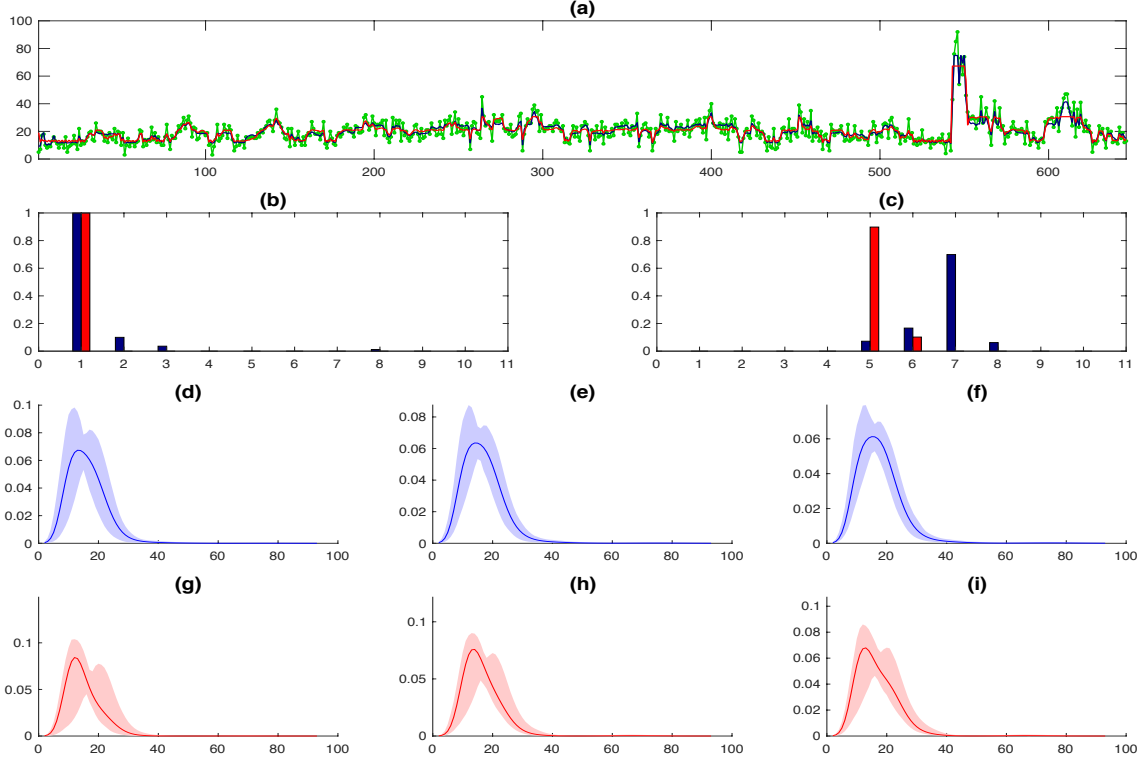


Figure 10: Results for the E.coli dataset: CTF-HOHMM in blue and HDP-HMM in red (a) posterior means super-imposed over the observed time series in green; (b) the inclusion probabilities of different lags; (c) the distribution of different number of states; (d), (e), (f) estimated one, two and three steps ahead predictive densities, respectively, and their 90% credible intervals by the CTF-HOHMM; (g), (h), (i) estimated one, two and three steps ahead predictive densities, respectively, and their 90% credible intervals by the HDP-HMM.

$[-1, 1]$ essentially across disjoint intervals, thus ensuring identifiability of these states. As in Yau *et al.* (2011), we also use a translated-mixture of Normals as our emission distribution with $S = 5$ local components. Experiments with larger values of S did not result in any practical difference in the results.

Figure 11 summarizes the results for the Coriell aCGH dataset obtained by the proposed CTF-HOHMM and the HDP-HMM. The CTF-HOHMM results suggest a higher order dependence with the first three lags being the important ones. This is reflective of the fact that copy number variations usually occur in clusters of adjacent locations. Panel (a) in Figure 11 suggests that the CTF-HOHMM provides a better fit to local variations in the data, better capturing focal aberrations (Fridlyand *et al.*, 2004) due to alterations in very narrow regions. The predictive densities estimated by the two methods also look quite different. For example, for one step ahead prediction, the HDP-HMM basically predicts a Normal copy number state. The CTF-HOHMM, on the other hand, assigns equal probabilities to having either a Normal copy number

or an increased copy number. It takes in account not just the immediately preceding location, which had a Normal copy number state, but also the variation in a few preceding locations which had amplified copy numbers.

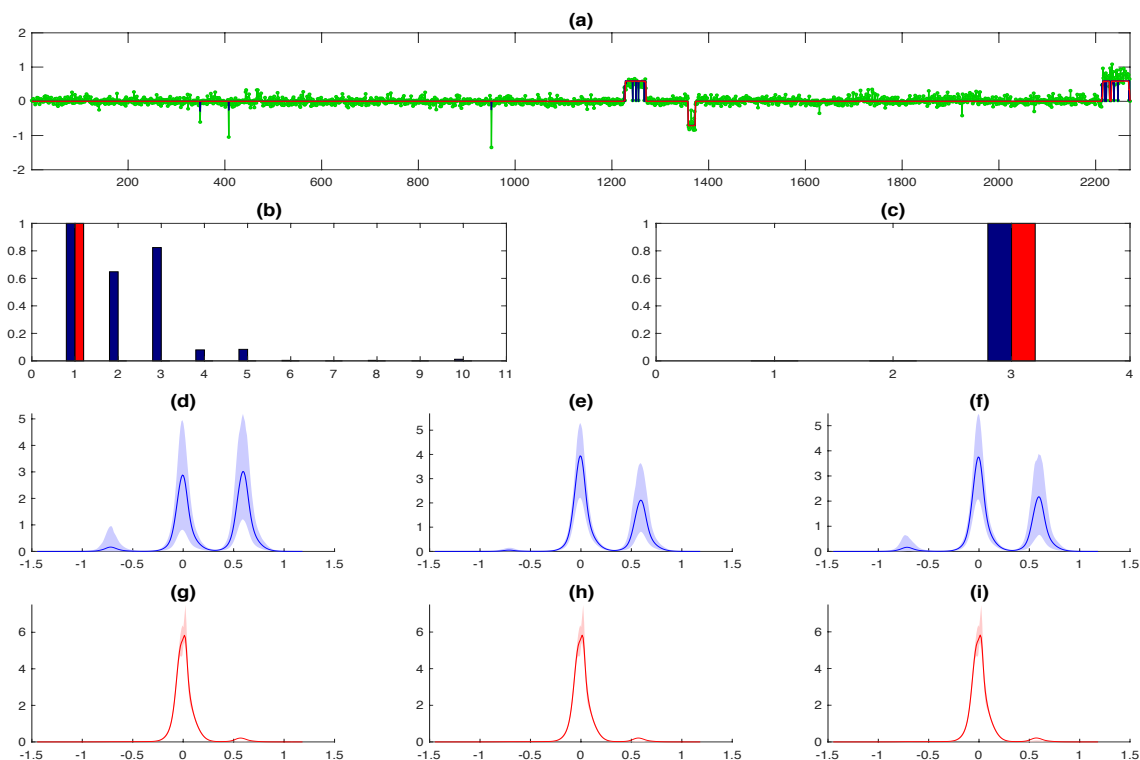


Figure 11: Results for the aCGH dataset: CTF-HOHMM in blue and HDP-HMM in red (a) posterior means super-imposed over the observed time series in green; (b) the inclusion probabilities of different lags; (c) the distribution of different number of states; (d), (e), (f) estimated one, two and three steps ahead predictive densities, respectively, and their 90% credible intervals by the CTF-HOHMM; (g), (h), (i) estimated one, two and three steps ahead predictive densities, respectively, and their 90% credible intervals by the HDP-HMM.

6 Discussion

We proposed a flexible yet parsimonious nonparametric Bayesian approach to higher order hidden Markov models that allows automated identification of the important lags. The celebrated HDP-HMM is obtained as a special case when the order is restricted to one and the soft sharing feature of the model is turned off. In simulation experiments, our method vastly out-performed the HDP-HMM in higher order settings. Remarkably, the improvements were also substantial in the first order cases which may be attributed to greater levels of data compression achievable by the proposed model.

The focus of this paper has been on higher order homogeneous HMMs, but the proposed methodology can be easily extended to nonhomogeneous cases where the transition dynamics and the emission distributions are allowed to be influenced by exogenous predictors. We are also pursuing the development of faster algorithms for online inference in HOHMMs that scale better with larger datasets. Additional important directions of ongoing research include extensions to other discrete state space dynamical systems, and models for spatial and spatio-temporal datasets.

Acknowledgments

This research was partially funded by Grant N00141410245 of the Office of Naval Research.

References

- Albert, J. and Chib, S. (1993). Calculating posterior distributions and modal estimates in Markov mixture models. *Journal of Business and Economic Statistics*, **11**, 1–15.
- Allman, E., Matias, C., and Rhodes, J. A. (2009). Identifiability of parameters in latent structure models with many observed variables. *Annals of Statistics*, **37**, 3099–3132.
- Azzalini, A. and Bowman, A. H. (1990). A look at some data on the Old Faithful geyser. *Journal of the Royal Statistical Society: Series C*, **39**, 357–365.
- Bae, K., Mallick, B. K., and Elvik, C. G. (2005). Prediction of protein interdomain linker regions by a hidden Markov model. *Bioinformatics*, **21**, 2264–2270.
- De Lathauwer, L., De Moore, B., and Vandewalle, J. (2000). A multilinear singular value decomposition. *SIAM Journal on Matrix Analysis and Applications*, **21**, 1253–1278.
- Ferguson, T. F. (1973). A Bayesian analysis of some nonparametric problems. *Annals of Statistics*, **1**, 209–230.
- Fox, E. B., Sudderth, E. B., Jordan, M. I., and Willsky, A. S. (2008). An HDP-HMM for systems with state persistence. *Proceedings of the 25th international conference on Machine learning*.
- Fridlyand, J., Snijders, A. M., Pinkel, D., Albertson, D. G., and Jain, A. N. (2004). Hidden Markov models approach to the analysis of array CGH data. *Journal of multivariate analysis*, **90**, 132–153.
- Gassiat, E., Cleynen, A., and Robin, S. (2015). Inference in finite state space non-parametric hidden Markov models and applications. *Statistics and Computing*, pages 10.1007/s11222-014-9523-8.

- George, E. and McCulloch, R. (1997). Approaches for Bayesian variable selection. *Statistica Sinica*, **7**, 339–373.
- Guha, S., Li, Y., and NewBerg, D. (2008a). Bayesian hidden Markov modeling of array CGH data. *Journal of the American Statistical Association*, **103**, 485–497.
- Guha, S., Li, Y., and Neuberg, D. (2008b). Bayesian hidden Markov modeling of array CGH data. *Journal of the American Statistical Association*, **103**, 485–497.
- Hamilton, J. E. (1990). Analysis of time series subject to changes in regime. *Journal of Econometrics*, **45**, 39–70.
- Ishwaran, H. and Zarepour, M. (2002). Exact and approximate sum representations for the Dirichlet process. *Canadian Journal of Statistics*, **30**, 158–182.
- Jääskinen, V., Xiong, J., Corander, J., and Koski, T. (2014). Sparse Markov chains for sequence data. *Scandinavian Journal of Statistics*, **41**, 639–655.
- Lennox, K. P., Dahl, D. B., Day, R., and Tsai, W. (2010). A Dirichlet process mixture of hidden Markov models for protein structure prediction. *Annals of Applied Statistics*, **4**, 916–942.
- Leroux, B. G. (1992). Maximum-likelihood estimation for hidden Markov models. *Stochastic Processes and their Applications*, **40**, 127–143.
- McDonald, S. and Zucchini, W. (1997). *Hidden Markov and other models for discrete-valued time series*. Chapman & Hall, London.
- Munkres, J. (1957). Algorithms for the assignment and transportation problems. *Journal of the Society of Industrial and Applied Mathematics*, **5**, 32–38.
- Rabiner, L. (1989). A tutorial on hidden Markov models and selected applications in speech recognition. *IEEE*, **77**, 257–286.
- Sarkar, A. and Dunson, D. B. (2016). Bayesian nonparametric modeling of higher-order Mmarkov chains. *Journal of the American Statistical Association*. Forthcoming.
- Scott, S. L. (2002). Bayesian methods for hidden Markov models recursive computing in the 21st century. *Journal of the American Statistical Association*, **97**, 337–351.
- Seifert, M., Gohr, A., Strickert, M., and Grosse, I. (2012). Parsimonious higher-order hidden Markov models for improved array-CGH analysis with applications to *Arabidopsis thaliana*. *PLoS Computational Biology*, **8**, 1–15.
- Sethuraman, J. (1994). A constructive definition of Dirichlet priors. *Statistica Sinica*, **4**, 639–650.
- Snijders, A. M., Nowak, N., Segreaves, R., Blackwood, S., Brown, N., Conroy, J., Hamilton, G., Hindle, A. K., Huey, B., Kimura, K., *et al.* (2001). Assembly of microarrays for genome-wide measurement of DNA copy number. *Nature Genetics*, **29**, 263–264.

- Teh, Y. W., Jordan, M. I., J., B. M., and M., B. D. (2006). Hierarchical Dirichlet processes. *Journal of the American Statistical Association*, **101**, 1566–1581.
- Thede, S. M. and Harper, M. P. (1999). A second-order hidden markov model for part-of-speech tagging. In *Proceedings of the 37th annual meeting of the Association for Computational Linguistics on Computational Linguistics*, pages 175–182. Association for Computational Linguistics.
- Tucker, L. (1966). Some mathematical notes on three-mode factor analysis. *Psychometrika*, **31**, 273–282.
- Yang, Y. and Dunson, D. B. (2016). Bayesian conditional tensor factorization for high-dimensional classification. *Journal of the American Statistical Association*, **111**, 656–669.
- Yau, C., Papaspiliopoulos, O., Roberts, G. O., and Holmes, C. (2011). Bayesian nonparametric hidden Markov models with applications in genomics. *Journal of the Royal Statistical Society, Series B*, **73**, 37–57.

Supplementary Materials for Bayesian Nonparametric Higher Order Hidden Markov Models

Abhra Sarkar

Department of Statistics and Data Sciences, University of Texas at Austin,
2317 Speedway D9800, Austin, TX 78712-1823, USA
abhra.sarkar@utexas.edu

and

David B. Dunson

Department of Statistical Science, Duke University,
Box 90251, Durham NC 27708-0251
dunson@duke.edu

S.1 Proof of Lemma 1

We refer to an HOHMM with transition probability tensor P , initial and stationary distribution $\boldsymbol{\pi}$, and emission distributions \mathbf{f} by HOHMM($P, \boldsymbol{\pi}, \mathbf{f}$). In the following, we write $\pi_{c_1, \dots, c_q} = \pi(c_1, \dots, c_q)$, $P_{c_{q+1}|c_1, \dots, c_q} = P(c_{q+1} | c_1, \dots, c_q)$ etc. The ergodicity of the underlying Markov chain implies that the stationary distribution $\boldsymbol{\pi}$ is unique with $\pi_{c_1, \dots, c_q} > 0$ for all $c_j \in \mathcal{C}, j = 1, \dots, q$. The joint distribution of $\mathbf{y}_{1:3q}$ under HOHMM($P, \boldsymbol{\pi}, \mathbf{f}$) is given by

$$\begin{aligned}
 p_{P, \mathbf{f}}(\mathbf{y}_{1:3q}) &= \sum_{c_1, \dots, c_{3q}} \pi_{c_1, \dots, c_q} P_{c_{q+1}|c_1, \dots, c_q} \cdots P_{c_{3q}|c_{2q}, \dots, c_{3q-1}} f_{c_1} \cdots f_{c_{3q}} \\
 &= \sum_{c_{q+1}, \dots, c_{2q}} \left\{ \sum_{c_1, \dots, c_q} \pi_{c_1, \dots, c_q} P_{c_{q+1}|c_1, \dots, c_q} \cdots P_{c_{2q}|c_q, \dots, c_{2q-1}} f_{c_1} \cdots f_{c_q} \right\} \\
 &\quad f_{c_{q+1}} \cdots f_{c_{2q}} \left\{ \sum_{c_{2q+1}, \dots, c_{3q}} P_{c_{2q+1}|c_{q+1}, \dots, c_{2q}} \cdots P_{c_{3q}|c_{2q}, \dots, c_{3q-1}} f_{c_{2q+1}} \cdots f_{c_{3q}} \right\} \\
 &= \sum_{c_{q+1}, \dots, c_{2q}} \pi_{c_{q+1}, \dots, c_{2q}} \left\{ \sum_{c_1, \dots, c_q} \frac{\pi_{c_1, \dots, c_q}}{\pi_{c_{q+1}, \dots, c_{2q}}} P_{c_{q+1}, \dots, c_{2q}|c_1, \dots, c_q} f_{c_1} \cdots f_{c_q} \right\} \\
 &\quad f_{c_2} \cdots f_{c_{q+1}} \left\{ \sum_{c_{2q+1}, \dots, c_{3q}} P_{c_{2q+1}, \dots, c_{3q}|c_{q+1}, \dots, c_{2q}} f_{c_{2q+1}} \cdots f_{c_{3q}} \right\} \\
 &= \sum_{c_{q+1}, \dots, c_{2q}} \pi_{c_{q+1}, \dots, c_{2q}} Q_{c_{q+1}, \dots, c_{2q}}^{(1)} Q_{c_{q+1}, \dots, c_{2q}}^{(2)} Q_{c_{q+1}, \dots, c_{2q}}^{(3)},
 \end{aligned}$$

where

$$\begin{aligned}
 Q_{c_{q+1}, \dots, c_{2q}}^{(1)} &= \sum_{c_1, \dots, c_q} (\pi_{c_1, \dots, c_q} / \pi_{c_{q+1}, \dots, c_{2q}}) P_{c_{q+1}, \dots, c_{2q} | c_1, \dots, c_q} f_{c_1} \dots f_{c_q}, \\
 Q_{c_{q+1}, \dots, c_{2q}}^{(2)} &= f_{c_2} \dots f_{c_{q+1}}, \quad \text{and} \\
 Q_{c_{q+1}, \dots, c_{2q}}^{(3)} &= \sum_{c_{2q+1}, \dots, c_{3q}} P_{c_{2q+1}, \dots, c_{3q} | c_{q+1}, \dots, c_{2q}} f_{c_{2q+1}} \dots f_{c_{3q}}.
 \end{aligned}$$

Also

$$\begin{aligned}
 P_{c_{q+1}, \dots, c_{2q} | c_1, \dots, c_q} &= P_{c_{q+1} | c_1, \dots, c_q} \dots P_{c_{2q} | c_q, \dots, c_{2q-1}}, \quad \text{and} \\
 P_{c_{2q+1}, \dots, c_{3q} | c_{q+1}, \dots, c_{2q}} &= P_{c_{2q+1} | c_{q+1}, \dots, c_{2q}} \dots P_{c_{3q} | c_{2q}, \dots, c_{3q-1}}.
 \end{aligned}$$

We have, for any $\{a_{c_{q+1}, \dots, c_{2q}} : a_{c_{q+1}, \dots, c_{2q}} \in \mathbb{R}, c_j \in \mathcal{C}, j = q+1, \dots, 2q\}$,

$$\begin{aligned}
 &\sum_{c_{q+1}, \dots, c_{2q}} a_{c_{q+1}, \dots, c_{2q}} Q_{c_{q+1}, \dots, c_{2q}}^{(1)} = 0 \\
 \Rightarrow &\sum_{c_1, \dots, c_q} \pi_{c_1, \dots, c_q} \left\{ \sum_{c_{q+1}, \dots, c_{2q}} \frac{a_{c_{q+1}, \dots, c_{2q}}}{\pi_{c_{q+1}, \dots, c_{2q}}} P_{c_{q+1}, \dots, c_{2q} | c_1, \dots, c_q} f_{c_1} \dots f_{c_q} \right\} f_{c_1} \dots f_{c_q} = 0 \\
 \Rightarrow &\sum_{c_{q+1}, \dots, c_{2q}} \frac{a_{c_{q+1}, \dots, c_{2q}}}{\pi_{c_{q+1}, \dots, c_{2q}}} P_{c_{q+1}, \dots, c_{2q} | c_1, \dots, c_q} = 0 \quad \text{for all } (c_1, \dots, c_q). \tag{S.1}
 \end{aligned}$$

The last line follows since the distributions $\{f_{c_1} \dots f_{c_q} : c_j \in \mathcal{C}, j = 1, \dots, q\}$ are linearly independent as $\{f_c : c \in \mathcal{C}\}$ are also so. $P_{c_{q+1}, \dots, c_{2q} | c_1, \dots, c_q} = p\{(c_{q+1}, \dots, c_{2q}) | (c_1, \dots, c_q)\}$ is the probability of moving from (c_1, \dots, c_q) to (c_{q+1}, \dots, c_{2q}) in q steps by a Markov chain with transition probability matrix \tilde{P} . Equation (S.1) can thus be written as

$$\tilde{P}^q \mathbf{b} = \mathbf{0}, \tag{S.2}$$

where \mathbf{b} is a vector of length C^q with elements $b_{c_{q+1}, \dots, c_{2q}} = a_{c_{q+1}, \dots, c_{2q}} / \pi_{c_{q+1}, \dots, c_{2q}}$ arranged in a specific order. By the assumption of Lemma 1, $\text{rank}(\tilde{P}^q) = \text{rank}(\tilde{P}) = C^q$. Equation (S.1) thus admits the unique solution $\mathbf{b} = \mathbf{0}$. This implies that $a_{c_{q+1}, \dots, c_{2q}} = 0$ for all (c_{q+1}, \dots, c_{2q}) and hence the distributions $\{Q_{c_{q+1}, \dots, c_{2q}}^{(1)} : c_j \in \mathcal{C}, j = q+1, \dots, 2q\}$ are linearly independent. Similarly,

$$\sum_{c_{q+1}, \dots, c_{2q}} a_{c_{q+1}, \dots, c_{2q}} Q_{c_{q+1}, \dots, c_{2q}}^{(3)} = 0 \quad \Rightarrow \quad \mathbf{a}^T \tilde{P}^q = \mathbf{0}^T, \tag{S.3}$$

where \mathbf{a} is a vector with elements $a_{c_{q+1}, \dots, c_{2q}}$. Equation (S.3) thus has the only solution $\mathbf{a} = \mathbf{0}$ and the distributions $\{Q_{c_{q+1}, \dots, c_{2q}}^{(3)} : c_j \in \mathcal{C}, j = q+1, \dots, 2q\}$ are linearly independent.

Let $\text{HOHMM}(P^*, \boldsymbol{\pi}^*, \mathbf{f}^*)$ be an HOHMM such that $p_{P, \mathbf{f}}(\mathbf{y}_{1:3q}) = p_{P^*, \mathbf{f}^*}(\mathbf{y}_{1:3q})$. Theorem 9 of Allman *et al.* (2009) then implies that there exists a permutation σ such that $f_{c_1}^* \dots f_{c_q}^* = f_{\sigma_1(c_1, \dots, c_q)} \dots f_{\sigma_q(c_1, \dots, c_q)}$, where $\sigma_j(c_1, \dots, c_q)$ is the j^{th} element of $\sigma(c_1, \dots, c_q)$. Since f_c^* and f_c

are probability distributions, for any pair (j, c_j) we have $f_{c_j}^* = f_{\sigma_j(c_1, \dots, c_q)}$ for all $c_\ell \in \mathcal{C}, \ell \neq j$, which implies $\sigma_j(c_1, \dots, c_q) = \sigma(c_j)$ for all $c_j \in \mathcal{C}, j = 1, \dots, q$, and hence $f_c^* = f_{\sigma(c)}$ for all $c \in \mathcal{C}$. Using Theorem 9 of Allman *et al.* (2009) again, we have, for all $(c_{2q+1}, \dots, c_{2q})$,

$$\begin{aligned} & \sum_{c_{2q+1}, \dots, c_{3q}} P_{c_{2q+1}, \dots, c_{3q}}^* | c_{q+1}, \dots, c_{2q} f_{c_{2q+1}}^* \cdots f_{c_{3q}}^* = \sum_{c_{2q+1}, \dots, c_{3q}} P_{c_{2q+1}, \dots, c_{3q} | \sigma(c_{q+1}), \dots, \sigma(c_{2q})} f_{c_{2q+1}} \cdots f_{c_{3q}} \\ \Rightarrow & \sum_{c_{2q+1}, \dots, c_{3q}} \left\{ P_{c_{2q+1}, \dots, c_{3q} | c_{q+1}, \dots, c_{2q}}^* - P_{\sigma(c_{2q+1}), \dots, \sigma(c_{3q}) | \sigma(c_{q+1}), \dots, \sigma(c_{2q})} \right\} f_{\sigma(c_{2q+1})} \cdots f_{\sigma(c_{3q})} = 0 \\ \Rightarrow & P_{c_{2q+1}, \dots, c_{3q} | c_{q+1}, \dots, c_{2q}}^* = P_{\sigma(c_{2q+1}), \dots, \sigma(c_{3q}) | \sigma(c_{q+1}), \dots, \sigma(c_{2q})} \text{ for all } (c_{2q+1}, \dots, c_{3q}). \end{aligned}$$

Summing successively over c_{3q}, \dots, c_{2q+2} and a change of variable names then gives

$$\Rightarrow P_{c_{q+1} | c_1, \dots, c_q}^* = P_{\sigma(c_{q+1}) | \sigma(c_1), \dots, \sigma(c_q)} \text{ for all } (c_1, \dots, c_q, c_{q+1}).$$

Finally, Theorem 9 of Allman *et al.* (2009) also implies that for all (c_{q+1}, \dots, c_{2q}) $\pi_{c_1, \dots, c_q}^* = \pi_{\sigma(c_1), \dots, \sigma(c_q)}$. This also follows from the fact that the stationary distribution $\boldsymbol{\pi}$ is uniquely determined by \tilde{P} . When $p_{P, \mathbf{f}}(\mathbf{y}_{1:3q}) = p_{P^*, \mathbf{f}^*}(\mathbf{y}_{1:3q})$, HOHMM($P, \boldsymbol{\pi}, \mathbf{f}$) and HOHMM($P^*, \boldsymbol{\pi}^*, \mathbf{f}^*$) are thus equivalent up to label swapping of the states which completes the proof of part 2 of Lemma 1.

S.2 Higher Order Chinese Restaurant Franchise

S.2.1 The Original CRF

We first review the original CRF (Teh *et al.* . 2006) before we describe how we adapted it to our HOHMM setting in the next subsection. Let there be J groups, each with N_j observations $\{y_{j,\ell}\}_{\ell=1}^{N_j}$ with a generative model as

$$\begin{aligned} \boldsymbol{\lambda}_0 & | \alpha_0 \sim \text{Dir}(\alpha_0/C, \dots, \alpha_0/C), \\ \boldsymbol{\lambda}_j & | \alpha, \boldsymbol{\lambda}_0 \sim \text{Dir}(\alpha \boldsymbol{\lambda}_0), \quad c_{j,\ell} | \boldsymbol{\lambda}_j \sim \text{Mult}\{\lambda_j(1), \dots, \lambda_j(C)\} \\ y_{j,\ell} & | \{\theta_c\}_{c=1}^C, c_{j,\ell} = k \sim f(\theta_k), \quad \theta_c \sim p_0. \end{aligned}$$

The model generating the labels $c_{j,\ell}$'s may be reformulated as

$$\begin{aligned} \boldsymbol{\lambda}_0 & | \alpha_0 \sim \text{Dir}(\alpha_0/C, \dots, \alpha_0/C), \\ G_j & = \sum_{k=1}^C \lambda_j(k) \delta_k, \quad \boldsymbol{\lambda}_j | \alpha, \boldsymbol{\lambda}_0 \sim \text{Dir}(\alpha \boldsymbol{\lambda}_0), \quad c_{j,\ell} | G_j \sim G_j. \end{aligned}$$

Another representation is given by

$$G_0 = \sum_{k=1}^C \lambda_0(k) \delta_k, \quad \boldsymbol{\lambda}_0 | \alpha_0 \sim \text{Dir}(\alpha_0/C, \dots, \alpha_0/C),$$

$$G_j = \sum_{\tau=1}^{\infty} \tilde{\lambda}_j(\tau) \delta_{\psi_{j,\tau}}, \quad \tilde{\lambda}_j \sim \text{SB}(\alpha), \quad \psi_{j,\tau} \sim G_0, \quad c_{j,\ell} | G_j \sim G_j.$$

A CRF arising from this generative model is as follows. Corresponding to the J groups, imagine J restaurants, each with infinitely many tables but finitely many dishes $\mathcal{C} = \{1, \dots, C\}$ on their globally shared menu. The ℓ^{th} customer belonging to the j^{th} group enters restaurant j , sits at a table $\tau_{j,\ell}$, and is served a dish $c_{j,\ell}$. While the restaurant assignments are predetermined by group memberships, the table assignment for the ℓ^{th} customer in restaurant j is chosen as $\tau_{j,\ell} \sim \tilde{\lambda}_j$, and each table τ is assigned a dish $\psi_{j,\tau} \sim \lambda_0$. Customers sitting at the same table thus all eat the same dish. Multiple tables may, however, be served the same dish, allowing two customers enjoying the same dish to be seated at different tables. Given $c_{j,\ell}$ and the corresponding table assignment $\tau_{j,\ell}$, $\psi_{j,\tau_{j,\ell}} = c_{j,\ell}$. See Figure S.1.

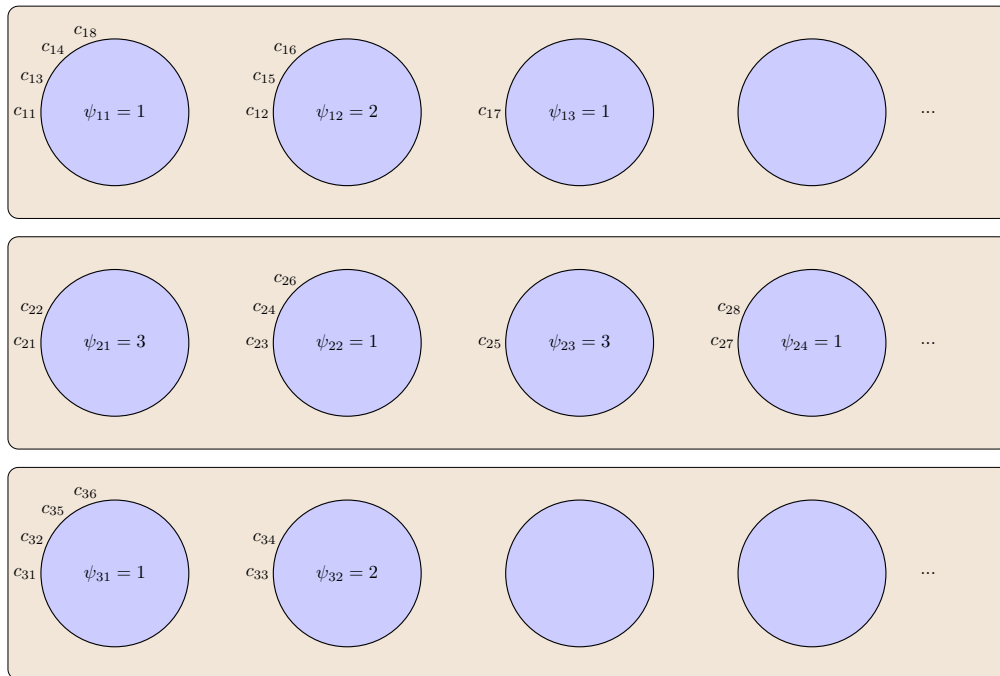


Figure S.1: The Chinese restaurant franchise.

Let $n_{j,\tau}$ denote the number of customers in restaurant j at table τ , $n_j(\psi)$ denote the number of customers in restaurant j eating the dish ψ , and n_j denote the total number of customers in restaurant j . Also, let $n_{j,\tau}(\psi)$ denote the number of customers in restaurant j at table τ eating dish ψ . Clearly, $n_{j,\tau}(\psi) > 0$ only when dish ψ is served at an occupied table τ . Finally, let $m_j(\psi)$ be the number of tables in restaurant j serving dish ψ , and m_j be the total number of occupied tables in restaurant j .

Given a posterior sample of the dish assignments, we can obtain a draw from the posterior of λ_j by noting that a-priori $\lambda_j \sim \text{Dir}\{\alpha\lambda_0(1), \dots, \alpha\lambda_0(C)\}$ and that $c_{j,\ell}$ for each j, ℓ is a draw from λ_j . The number of different $c_{j,\ell}$'s that are associated with a specific dish c thus

equals the total number of customers in the restaurant j eating the dish c , that is, $n_j(c)$. Using Dirichlet-Multinomial conjugacy, we then have

$$(\boldsymbol{\lambda}_j \mid \alpha, \boldsymbol{\lambda}_0, \mathbf{n}, \boldsymbol{\zeta}) \sim \text{Dir}\{\alpha\lambda_0(1) + n_j(1), \dots, \alpha\lambda_0(C) + n_j(C)\}.$$

Likewise, given a sample $(\boldsymbol{\tau}, \boldsymbol{\psi})$ of the table and the dish assignments, we can obtain a draw from the posterior of $\boldsymbol{\lambda}_0$ by noting that a-priori $\boldsymbol{\lambda}_0 \sim \text{Dir}(\alpha_0/C, \dots, \alpha_0/C)$ and that $\psi_{j,\tau}$ for each τ is a draw from $\boldsymbol{\lambda}_0$. The number of different $\psi_{j,\tau}$'s that are associated with a specific dish ψ is precisely the number of tables in the restaurant j that served the dish ψ , that is, $m_j(\psi)$. The total number of tables serving dish ψ across all restaurants is therefore $m_0(\psi) = \sum_j m_j(\psi)$. Using Dirichlet-Multinomial conjugacy, we then have

$$(\boldsymbol{\lambda}_0 \mid \mathbf{m}, \boldsymbol{\zeta}) \sim \text{Dir}\{\alpha_0/C + m_0(1), \dots, \alpha_0/C + m_0(C)\}.$$

The table assignments $\boldsymbol{\tau}$ are also latent. To sample $\boldsymbol{\tau}$ from the posterior, we first marginalize out their prior $\tilde{\boldsymbol{\lambda}}_j \sim \text{SB}(\alpha)$ to obtain

$$(\tau_{j,\ell} \mid \alpha, \boldsymbol{\tau}_j^{-\ell}) \sim \sum_{\tau \in \mathcal{S}_{j,\tau}^{-\ell}} \frac{n_{j,\tau}^{-\ell}}{n_j - 1 + \alpha} \delta_\tau + \frac{\alpha}{n_j - 1 + \alpha} \delta_{\tau_{new}},$$

where $n_{j,\tau}^{-\ell}$ denotes the number of customers sitting at table τ in restaurant j excluding the ℓ^{th} customer, $\mathcal{S}_{j,\tau}^{-\ell}$ denotes the set of unique values in $\boldsymbol{\tau}_j^{-\ell} = \{\tau_{j,s} : s = 1, \dots, n_j, s \neq \ell\}$ and τ_{new} is a generic for any new value of τ not in $\mathcal{S}_{j,\tau}^{-\ell}$. The distribution of the table assignment $\tau_{j,\ell}$ given $\boldsymbol{\tau}_j^{-\ell}$ and the dish assignments $\boldsymbol{\psi}$ may then be obtained as

$$\begin{aligned} p(\tau_{j,\ell} = \tau \mid \psi_{j,\tau} = \psi, \alpha, \boldsymbol{\psi}_j^{-\ell}, \boldsymbol{\tau}_j^{-\ell}, \boldsymbol{\lambda}_0) &\propto n_{j,\tau}^{-\ell} \delta_\tau \quad \text{if } \tau \in \mathcal{S}_{j,\tau}^{-\ell}, \\ p(\tau_{j,\ell} = \tau_{new} \mid \psi_{j,\tau_{new}} = \psi, \alpha, \boldsymbol{\psi}_j^{-\ell}, \boldsymbol{\tau}_j^{-\ell}, \boldsymbol{\lambda}_0) &\propto \alpha \lambda_0(\psi) \quad \text{if } \tau_{new} \notin \mathcal{S}_{j,\tau}^{-\ell}, \end{aligned}$$

where $\boldsymbol{\psi}_j^{-\ell} = \{\psi_{j,\tau_{j,s}} : s = 1, \dots, n_j, s \neq \ell\}$. Since these assignments are restricted only to tables serving the dish ψ , the distribution reduces to

$$(\tau_{j,\ell} \mid \psi_{j,\tau_{j,\ell}} = \psi, \alpha, \boldsymbol{\psi}_j^{-\ell}, \boldsymbol{\tau}_j^{-\ell}, \boldsymbol{\lambda}_0) \sim \sum_{\tau \in \mathcal{S}_{j,\tau}^{-\ell}(\psi)} \frac{n_{j,\tau}^{-\ell}(\psi)}{n_j(\psi) - 1 + \alpha \lambda_0(\psi)} \delta_\tau + \frac{\alpha \lambda_0(\psi)}{n_j(\psi) - 1 + \alpha \lambda_0(\psi)} \delta_{\tau_{new}},$$

where $\mathcal{S}_{j,\tau}^{-\ell}(\psi)$ denotes the set of unique values in $\boldsymbol{\tau}_j^{-\ell}(\psi) = \{\tau_{j,s} : s = 1, \dots, n_j, s \neq \ell, \psi_{j,\tau_{j,s}} = \psi\}$, $n_{j,\tau}^{-\ell}(\psi)$ denotes the number of customers sitting at table τ in restaurant j and enjoying the dish ψ excluding the ℓ^{th} customer, and τ_{new} is a generic for any new value of τ not in $\mathcal{S}_{j,\tau}^{-\ell}(\psi)$. This distribution can be identified with a marginalized conditional distribution of assignments of $n_j(\psi)$ observations to different components in a $\text{SB}\{\alpha \lambda_0(\psi)\}$. The full conditional for $\boldsymbol{\lambda}_0$ given $(\boldsymbol{\psi}, \boldsymbol{\tau})$ depends on the table assignments only via $m_j(\psi)$ which can be obtained from the table assignments $\boldsymbol{\tau}_j$.

Alternatively, for each of the $n_j(\psi)$ customers in restaurant j enjoying the dish ψ , let $m_{j,\ell}(\psi) = 0$ if the ℓ^{th} customer sits at an already occupied table, and $m_{j,\ell}(\psi) = 1$ if the ℓ^{th} customer goes to a new table. Then, $m_j(\psi) = \sum_{\ell=1}^{n_j(\psi)} m_{j,\ell}(\psi)$. Using properties of a $\text{SB}\{\alpha\lambda_0(\psi)\}$ distribution, we then have

$$\{m_{j,\ell}(\psi) \mid \mathbf{m}_j^{\ell-1}(\psi), \alpha, \boldsymbol{\lambda}_0\} \sim \frac{\ell-1}{\ell-1+\alpha\lambda_0(\psi)}\delta_0 + \frac{\alpha\lambda_0(\psi)}{\ell-1+\alpha\lambda_0(\psi)}\delta_1,$$

where $\mathbf{m}_j^{\ell-1}(\psi) = \{m_{j,s}(\psi) : s = 1, \dots, \ell-1\}$. We can then sample the $m_{j,\ell}(\psi)$'s from the posterior by sequentially sampling them as

$$[\{m_{j,\ell}(\psi)\}_{\ell=1}^{n_j(\psi)} \mid \alpha, \boldsymbol{\lambda}_0] \sim \prod_{\ell=1}^{n_j(\psi)} \text{Bernoulli} \left\{ \frac{\alpha\lambda_0(\psi)}{\ell-1+\alpha\lambda_0(\psi)} \right\}.$$

S.2.2 Higher Order CRF for CTF-HOHMM

While customers in the CRF of the HDP are pre-partitioned into restaurants based on their fixed group assignments, in our HOHMM setting the restaurant assignments are latent and hence are also sampled. Specifically, they are determined by the labels $z_{j,t}$'s - when $(z_{1,t}, \dots, z_{q,t}) = (h_1, \dots, h_q)$, the customer enters the $(h_1, \dots, h_q)^{\text{th}}$ restaurant. There are thus a total of $\prod_{j=1}^q k_j$ restaurants.

We recall that the j^{th} lag c_{t-j} is important in predicting the dynamics of c_t only when $k_j > 1$. In the culinary analogy, the j^{th} lag is thus important if it has restaurants named (labeled) after it.

The total number of customers entering the $(h_1, \dots, h_q)^{\text{th}}$ restaurant is now $n_{h_1, \dots, h_q} = \sum_t 1\{z_{1,t} = h_1, \dots, z_{q,t} = h_q\}$. Among them, the number of customers eating the dish c is $n_{h_1, \dots, h_q}(c) = \sum_t 1\{z_{1,t} = h_1, \dots, z_{q,t} = h_q, c_t = c\}$. Using Dirichlet-Multinomial conjugacy, we then have

$$(\boldsymbol{\lambda}_{h_1, \dots, h_q} \mid \boldsymbol{\zeta}) \sim \text{Dir}\{\alpha\lambda_0(1) + n_{h_1, \dots, h_q}(1), \dots, \alpha\lambda_0(C) + n_{h_1, \dots, h_q}(C)\}.$$

We next define, for each $\ell = 1, \dots, n_{h_1, \dots, h_q}(c)$, $m_{\ell, h_1, \dots, h_q}(c) = 0$ if the customer sits at an already occupied table and $m_{\ell, h_1, \dots, h_q}(c) = 1$ if the customer goes to a new table. Then, we can sample $\{m_{\ell, h_1, \dots, h_q}(c)\}_{\ell=1}^{n_{h_1, \dots, h_q}(c)}$ from the posterior by sampling them sequentially from

$$\{m_{\ell, h_1, \dots, h_q}(c)\}_{\ell=1}^{n_{h_1, \dots, h_q}(c)} \mid \boldsymbol{\zeta} \sim \prod_{\ell=1}^{n_{h_1, \dots, h_q}(c)} \text{Bernoulli} \left\{ \frac{\alpha\lambda_0(c)}{\ell-1+\alpha\lambda_0(c)} \right\}.$$

Then, $m_{h_1, \dots, h_q}(c) = \sum_{\ell=1}^{n_{h_1, \dots, h_q}(c)} m_{\ell, h_1, \dots, h_q}(c)$ gives the number of occupied tables serving the dish c in the $(h_1, \dots, h_q)^{\text{th}}$ restaurant.

The table assignments in restaurants (h_1, \dots, h_q) follow $\boldsymbol{\lambda}_0$. Letting $m_0(c) = \sum_{h_1, \dots, h_q} m_{h_1, \dots, h_q}(c)$ denote the total number of tables serving dish c across all such restaurants, we can update

λ_0 using Dirichlet-Multinomial conjugacy as

$$\{\lambda_0(1), \dots, \lambda_0(C)\} \mid \zeta \sim \text{Dir}\{\alpha_0/C + m_0(1), \dots, \alpha_0/C + m_0(C)\}.$$

S.3 Sampling Prior Hyper-parameters

The full conditional for the hyper-parameter α in the original CRF can be derived assuming a $\text{Ga}(a, b)$ prior and adapting to West (1992). Following Antoniak (1974), integrating out λ_0 , we have $p(m_j \mid \alpha, n_j) = \alpha^{m_j} s^*(n_j, m_j) \Gamma(\alpha) / \Gamma(\alpha + n_j)$, where $s^*(n, v)$ are Stirling numbers of the first kind. Letting $\mathbf{n} = \{n_j\}_{j=1}^J$, $\mathbf{m} = \{m_j\}_{j=1}^J$ with $v = \sum_{j=1}^J m_j$, since the restaurants are conditionally independent, we have

$$\begin{aligned} p(\alpha \mid \mathbf{m}, \mathbf{n}, \zeta) &\propto p_0(\alpha \mid a, b) p(\mathbf{m} \mid \alpha, \mathbf{n}) \propto \exp(-\alpha b) (\alpha)^{a-1} \prod_{j=1}^J \left\{ (\alpha)^{m_j} \frac{\Gamma(\alpha)}{\Gamma(\alpha + n_j)} \right\} \\ &\propto \exp(-\alpha b) (\alpha)^{a+v-1} \prod_{j=1}^J \left\{ \frac{(\alpha + n_j) \text{Beta}(\alpha + 1, n_j)}{\alpha \Gamma(n_j)} \right\} \\ &\propto \exp(-\alpha b) (\alpha)^{a+v-1} \prod_{j=1}^J \left\{ \left(1 + \frac{n_j}{\alpha}\right) \int r_j^\alpha (1 - r_j)^{n_j-1} dr_j \right\} \\ &\propto \exp(-\alpha b) (\alpha)^{a+v-1} \prod_{j=1}^J \left\{ \sum_{s_j=0}^1 \left(\frac{n_j}{\alpha}\right)^{s_j} \int r_j^\alpha (1 - r_j)^{n_j-1} dr_j \right\}. \end{aligned}$$

Treating $\mathbf{r} = \{r_j\}_{j=1}^J$, $\mathbf{s} = \{s_j\}_{j=1}^J$ as auxiliary variables, we have

$$p(\alpha, \mathbf{r}, \mathbf{s} \mid \zeta) \propto \exp(-\alpha b) (\alpha)^{a+v-1} \prod_j \left\{ \left(\frac{n_j}{\alpha}\right)^{s_j} r_j^\alpha (1 - r_j)^{n_j-1} \right\}.$$

The full conditionals for α , r_j and s_j are then obtained in closed forms as

$$(\alpha \mid \zeta) \sim \text{Ga}(a + v - s, b - \log r), \quad (r_j \mid \zeta) \sim \text{Beta}(\alpha + 1, n_j), \quad (s_j \mid \zeta) \sim \text{Bernoulli}\left(\frac{n_j}{n_j + \alpha}\right),$$

where $\log r = \sum_{j=1}^J \log r_j$, and $s = \sum_{j=1}^J s_j$.

To sample the hyper-parameter α in the HOHMM setting, we mimic the derivations in the CRF and introduce auxiliary variables r_{h_1, \dots, h_q} and s_{h_1, \dots, h_q} for each h_1, \dots, h_q . Let $\mathbf{n}_0 = \{n_{h_1, \dots, h_q}\}$; $\mathbf{m}_0, \mathbf{r}_0, \mathbf{s}_0$ are similarly defined. It can then follows that

$$\begin{aligned} \alpha \mid \zeta &\sim \text{Ga}(a_0 + m_0 - s_0, b_0 - \log r_0), \\ r_{h_1, \dots, h_q} \mid \zeta &\sim \text{Beta}(\alpha + 1, n_{h_1, \dots, h_q}), \\ s_{h_1, \dots, h_q} \mid \zeta &\sim \text{Bernoulli}\left(\frac{n_{h_1, \dots, h_q}}{n_{h_1, \dots, h_q} + \alpha}\right), \end{aligned}$$

where $m_0 = \sum_{y_t} \sum_{y_{t-1}} \sum_{h_1, \dots, h_q} m_{h_1, \dots, h_q}(c_t)$, $\log r_0 = \sum_{h_1, \dots, h_q} \log r_{h_1, \dots, h_q}$, and $s_0 = \sum_{h_1, \dots, h_q} s_{h_1, \dots, h_q}$.

Additionally, with an exponential prior $\varphi_0 \exp(-\varphi_0 \varphi)$ on φ , its full conditional is

$$\varphi \mid \zeta \sim \exp\{-(\varphi_0 + \sum_j j k_j) \varphi\}.$$

In simulation experiments and real data applications, we set the prior hyper-parameters at $a_0 = b_0 = 1$ and $\varphi_0 = 2$. The results were highly robust to these choices.

References

- Altman, R. M. (2007). Mixed hidden Markov models: an extension of the hidden Markov model to the longitudinal data setting. *Journal of the American Statistical Association*, 102, 201-210.
- Antoniak, C. E. (1974). Mixtures of Dirichlet processes with applications to Bayesian non-parametric problems. *Annals of Statistics*, 2, 1152-1174.
- Teh, Y. W., Jordan, M. I., Beal, M. J., and Blei, D. M. (2006). Hierarchical Dirichlet processes. *Journal of the American Statistical Association*, 101, 1566-1581.
- West, M. (1992). Hyperparameter estimation in Dirichlet process mixture models. Institute of Statistics and Decision Sciences, Duke University, Durham, USA, Technical report.